UNIVERSITÀ
DEGLI STUDI
DI PADOVA

DIPARTIMENTO
DI INGEGNERIA
DELL'INFORMAZIONE

DIPARTIMENTO DI INGEGNERIA DELL'INFORMAZIONE

CORSO DI LAUREA MAGISTRALE IN BIOINGEGNERIA

"INTRODUCING CARBOHYDRATES SUGGESTIONS AND CORRECTIVE BOLUSES ADMINISTRATIONS IN ARTIFICIAL PANCREAS BY MODEL PREDICTIVE CONTROL"

Relatore: Prof. Simone Del Favero

Laureando: Lorenzo Cester

Correlatore: Dott. Jacopo Pavan

ANNO ACCADEMICO 2022 – 2023

Data di laurea 10 Luglio 2023

Contents

Abstract

Type 1 diabetes (T1D) is characterized by the absence of insulin production and thus by an impaired glycaemia control. T1D therapy consists in providing insulin to the patient, aiming to maintain the blood glucose level in euglycaemia (i.e., between 70 and 180 $\frac{\text{mg}}{\text{dl}}$), counteracting hyperglycaemia, but without incurring in hypoglycaemic events, which can lead to severe consequences in the short term. This is not trivial, due to disturbing factors and given the pharmacokinetics and pharmacodynamics[1] of exogenous insulin.

The Artificial Pancreas (AP) is a new technology for the automation and the optimization of basal insulin administration, which works by a closed-loop algorithm that controls the functioning of an insulin pump, basing on the measurements provided by a glucose sensor. The objective of this work is to improve the quality of glycaemia control, by adding in AP the possibility to suggest carbohydrates assumptions and the administration of corrective insulin boluses, by using the Model Predictive Control (MPC) algorithm. The idea is to strengthen the counteraction of hypo- and hyperglycaemia, respectively.

To model the quantity of CHO to be suggested and the capability of the algorithm to choose whether to deliver a bolus or not, a series of Boolean support variables is needed and has to be included in the control problem. Therefore, our approach involves the resolution of a Mixed Integer Quadratic Programming (MIQP) problem, which the MPC's control problem can be reformulated as.

To evaluate the performances of the resultant system (the triple-action MPC AP), we resort to the *UVa/Padova T1D Simulator®*, an accurate model of a T1D patient's metabolism, which was accepted by the U.S. FDA (Food and Drug Administration) as a substitute of animal trials for preclinical testing of T1D therapies, and is integrated with a population of realistic virtual subjects to perform the trials on. We compare our approach with a state-of-the-art strategy (the single-action MPC AP), which only manages the basal insulin delivery, and an advanced technique (the dual-action MPC AP), which, in addition, can suggest carbohydrates intakes.

The results show how the triple-action MPC AP outperforms both the single-action- and the dual-action MPC AP, with an increment of the average time in euglycaemia of more than 9% and almost 3%, respectively, with the optimal parametrization. Adopting a suboptimal tuning,

[1] The pharmacokinetics (PK) of a drug are the quantitative description of how the body interacts with the substance, for the entire duration of the exposure (i.e. "what the body does to the drug"). The pharmacodynamics (PD) are the description of the biochemical, physiologic and molecular effects the drug has on the body (i.e. "what the drug does to the body").

inferred by using hyperparameters' regression models, our approach still outperforms the single-action technique, with an increase of the time in euglycaemia of almost 5%, and shows slightly better performances with respect to the dual-action MPC AP, as well.

I. Introduction

Type 1 diabetes (T1D) is an autoimmune[2] disease causing the destruction of the beta-cells in the Langerhans islets in pancreas. The task of these cells is to produce insulin, which is the fundamental hormone in the utilization process of glucose, to generate ATP[3] for most of the tissues, and for the regulation of glucose level in blood (glycaemia) as well. Therefore, the lack of the endogenous insulin in T1D patients leads to ketoacidosis[4], since lipids are much more employed as an alternative source of energy, but also to an impaired glycaemia regulation. Glucose remains in blood within anomalous levels, reaching values over $180\ \frac{\text{mg}}{\text{dl}}$ (hyperglycaemia), that is a condition which, if prolonged in time, can cause micro- and macro-vascular complications and thus diabetic retinopathy, an increased risk of heart disease, but also neuropathy, nephropathy, and several other problems. Therefore, T1D therapy consists in supplying exogenous insulin (adopting artificial substitutes) in such a way to adjust the blood glucose (BG) level and to try to maintain it in euglycaemia, i.e. under $180\ \frac{\text{mg}}{\text{dl}}$ but over $70\ \frac{\text{mg}}{\text{dl}}$ as well. Lower levels, referred as hypoglycaemia, indeed, are even more dangerous, since they lead to short-term critical issues, namely seizure, coma or even death if not promptly treated, and must be avoided as much as possible [1-2]. This is not a trivial task, due to the external sources of variability and disturbance, namely meals, physical exercise and stress, and to the fact that it must be taken into account that exogenous insulin acts gradually and with a certain delay, from the time of infusion [3-4].

The traditionally adopted therapy for T1D involves several time-sparse manual insulin administrations, via insulin pens, and BG measurements by fingerstick devices, along the day. In detail, the patient is required to take a predefined quantity of insulin shortly before each meal (meal bolus), calculated with an empirical formula that takes into account the estimated amount of carbohydrates (CHO) in the meal, the difference between the measured glycaemia and the desired value, and the insulin-on-board[5]. In addition, whenever he or she feels that is undergoing a hypo- or hyperglycaemic event, he or she should measure the blood glucose level

---

[2] Autoimmune pathologies are characterized by a dysfunction of the immune system, that induces the organism to attack its own tissues. The underlying causes of these diseases are still not known, therefore they are particularly hard to be addressed.

[3] Adenosine triphosphate (ATP) is the molecule that acts like the source of energy for the cells, to perform any biological task.

[4] Ketoacidosis is a complication of diabetes, characterized by a reduction of the hematic PH, caused by a major release of acid components in blood due to an excessive use of lipids for ATP production. This can provoke dehydration, polyuria, polydipsia, hypotension and arrhythmias [1].

[5] Namely the insulin which is still active in the body at a given time, from a previous administration. This can be computed with a heuristic method, as reported in [5].

and perform a corrective action, i.e. take a certain amount of CHO or insulin, respectively. An improvement came from the introduction in the market of continuous glucose monitoring (CGM) sensors, that allow to oversee the glucose level in the interstitial zone automatically and in a practically constant way, and pumps for the continuous subcutaneous insulin infusion (CSII). Here, the meaning of "continuous" is to be intended as the fact that they both work at a relatively high frequency; in particular, the sampling time of the sensor is 1-5 minutes [6]. The combination of a CGM sensor with a CSII pump, being manually driven by the patient, form the set-up for the so-called sensor-augmented-pump (SAP) therapy. However, the crucial issue of the SAP strategy, as well as for the mentioned traditional approach, is that every control action has to be managed by the patient and, therefore, the effectiveness of the therapy heavily depends on his or her diligence and concentration, which must be constant. For this reason, a manual approach can be particularly burdensome for the individual and is not really robust, leaving room for further improvement [7].

In the perspective of automatizing and optimizing insulin administration, the Artificial Pancreas (AP) technology is emerged. It works by a closed-loop control algorithm, which is in charge of regulating the functioning of a CSII pump, on the basis of the measures provided by a CGM sensor, trying to mimic the behaviour of a real pancreas [8-9]. In this way, there is a software that fulfils, in a potentially optimized way, what otherwise should be performed by the patient, whose burden is thus significantly lower. Several algorithms have been examined for the AP controller (fuzzy logic, PID) [10-11], but the most successful and so the most adopted one is the Model Predictive Control (MPC) [12-14], mainly because it employs a predictive reasoning and for its capability to handle constraints on the control variables. This is the technique adopted in the current work.

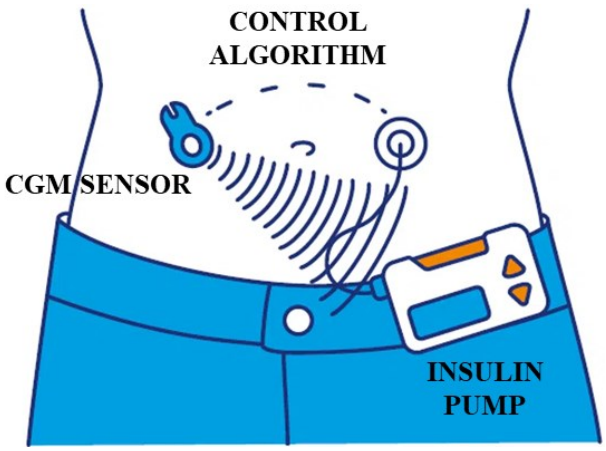

Figure 1. The AP architecture.

Most of the state-of-art systems are single-hormone APs [15-16], i.e. the algorithm they work with controls a unique variable, precisely the basal pump insulin infusion. Therefore, the glycaemia can be controlled only by being reduced (since this is the effect the insulin has on it), but there is not any other variable to get the opposite outcome, i.e. to actively promote a glucose increase, which significantly limits how much aggressively the hyperglycaemic events can be tackled, without incurring in hypoglycaemia. A state-of-art solution to try to overcome this issue is to suggest the assumption of fast-acting CHO when a hypoglycaemic event is detected or predicted to happen (emergency hypotreatment, i.e. against hypoglycaemia); this helps in avoiding moderate glucose drops, but it has to be noticed that this is a mere emergency measure and it is not coordinated with the control action on the insulin infusion, being managed by a module that is independent from the control algorithm [17].

In [17], exploiting an important feature of the MPC that is the capability to manage more control variables simultaneously, Pavan et al. propose an new technique, to be referred as dual-action MPC AP (in short, dualMPC): a single-hormone MPC AP, or singleMPC in brief (precisely an AP working with a MPC that manages only the basal insulin infusion), which controls an additional variable representing extra-CHO intakes. The strength of this algorithm comes from the fact the CHO intakes, to be suggested to the patient mainly as hypotreatments, are planned proactively in synergy with the insulin control. However, an issue affecting this strategy is that the patient is heavily involved in the control loop (human-in-the-loop problem): the suggested carbohydrates cannot be administered automatically if not in a hospital environment, since they can be infused intravenously but not subcutaneously; therefore, the subject is in charge of manually assume them. To lighten the extra-burden the patient has, some constraints are applied: the suggested CHO amounts have to be quantized among a few values, to ease their assumption and to reduce the risk of carb-counting errors; the CHO suggestions have to be sparse in time and there is a maximum number of them that can be given in a day; in addition, there can be "do-not-disturb" time periods, when no extra-CHO intakes can be suggested [17].

In this work we aim to achieve a further improvement for AP, exploring the possibility for the algorithm to manage the delivery of extra corrective insulin boluses, mainly as hypertreatments (i.e., against hyperglycaemia). There is consensus in the clinical community that the additional administration of insulin boluses may improve control, since they appear essential to counteract persistent hyperglycaemia; indeed, boluses are (variable) quantities of insulin that are released all at once and so are expected to have a large impact on glycaemia. This option has already been investigated, coupling the corrective boluses management with the basal insulin infusion control, however making use of modules independent from the controller [18] or heuristic

methods [19] for the boluses' definition, basing on a mere reactive (not proactive) reasoning. Conversely, our goal is to obtain an innovative algorithm, adding to the dualMPC AP the capability to proactively plan also the administration of the corrective boluses, including them with a third control variable. In this way, we aim to achieve a method that helps in counteracting any hyperglycaemic peak, persistent or not, much more aggressively and effectively, still relying on the capability of the algorithm to suggest CHO intakes to avoid dangerous glucose drops that could arise as a consequence, and so to have a more stable BG trend. Even if there can be an ambiguity between the basal insulin (i.e. the first control variable) and the corrective boluses (since they both consist in insulin), the latter have to be intended as something separated (and to be subject to different constraints) with respect to the former, but still in synergy with all the other manipulated variables. Since they can possibly have a great impact on glycaemia and thus can significantly influence the physical state of the individual, their administration should be confirmed by him or her, if he or she feels to be in the right condition for that. For this reason, they must be bounded to the constraint of the sparsity in time as well, in order to contain the patient's burden. Analogously to the definition proposed by Pavan et al. in [17], our system will be called in the following as triple-action MPC AP (or tripleMPC in short).

We compare our approach both with a state-of-the-art strategy, which is the singleMPC, and with the dualMPC, to be considered as an advanced technique. In order to test the performances of the three versions of the MPC AP that we consider, a series of trials, on a given population of T1D patients, has to performed. At the state-of-the-art, the easiest and most convenient option is *in-silico* testing; in our work, for this purpose we exploit the latest version of the *UVa/Padova T1D Simulator®* (v. 2013) [20], a large-scale and accurate model of the T1D metabolic subsystem. Indeed, it was accepted by the U.S. Food and Drug Administration (FDA) as a substitute of animal testing for preclinical trials for T1D therapies evaluation, thus representing a less expensive, less complicated, more rapid, and ethical alternative way for testing. Therefore, now it is a well-established tool for this scope in the scientific literature [20-21]. The parameters of the model this simulator is based on are not unique, but a dataset of 100 virtual T1D patients, each one representing a different set of parameters and spanning the variability observed in a real T1D population, is available and comes with the simulator. In the simulation scenario we adopt, the *UVa/Padova T1D* simulator is integrated with a model simulating the functioning of a real CGM sensor, a patient decisions' simulator [22], which models the meal announcement (that indeed must be provided by him or her) and the administration of the emergency hypotreatments, and of course a module where the controller is implemented, thus replicating the AP logic architecture as well.

MPC is a model-based technique, as its name may suggest. For the examined MPC APs, we adopt a linearized version of the *UVa/Padova T1D* system, in order to achieve a trade-off between the accuracy of the resultant model and its simplicity, which makes the problem more robust and lowers the computational cost. For major feasibility, we consider uniquely the model of the average virtual patient, for any tested individual.

1.1. Thesis organization

The thesis will be structured as follows. Section II focuses on the methods and particularly on the implementation of the single-, the dual- and the tripleMPC. In section III the experimental set-up is discussed, describing in detail the mentioned simulator, the simulation scenario and the metrics adopted to assess the algorithms' performances. In section IV, we explain the tuning procedure for the MPCs' hyperparameters. In section V the results are shown and properly discussed. The conclusions and some final remarks are reported in section VI. An appendices' section containing further useful details is present as well.

II. Methods

The control problem we aim to solve consists in regulating the blood glucose $BG(k)$, but in true what the AP disposes of are measurements of the patient's interstitial glucose $g(k)$, provided by the CGM sensor every 5 minutes. Therefore, what we aim to do is to keep $g(k)$ as close as possible to a suitable target value g_0, acting against several disturbances, the main being represented by the meals, and unexplained metabolic fluctuations; in our work we set $g_0 = 120\ \frac{\text{mg}}{\text{dl}}$. We assume that the information about the incoming meal's CHO amount (meal announcement) is provided by the patient to the system; for this reason, the meal disturbance $d(k)$ can be considered measurable, but what the AP disposes of is actually an estimate of it $\hat{d}(k)$, possibly affected by errors [17].

The MPC solves the problem explained above by following the Receding Prediction Horizon strategy [23]. At each time step, it considers the time interval comprehending the current step and the PH future ones, where PH stands for Prediction Horizon and is a settable constant. It thus searches for the optimal sequence of control actions for the current time and the $PH - 1$ steps ahead, between all the possible ones. Each element of the mentioned sequence is computed taking into account the correspondent predicted response of the system, i.e. for the subsequent time step[6] within the prediction horizon; therefore, the system's output g is forecasted for the PH future steps. Finally, according to the receding horizon policy, rather than using the entire calculated sequence, only its first element is applied, then waiting for the next CGM sensor's measurement; this is what makes the MPC strategy a closed-loop approach. The optimal control actions' sequence is established by minimizing a cost function, comprehending the terms mentioned above (i.e. the unknown sequence of control variables and the correspondent system's responses); consequently, the control problem is reconducted to an optimization one. The predictions about g are computed exploiting a model of the T1D metabolic subsystem (this is why MPC is a model-based algorithm), to be initialized at each step with the system's current state x, to be estimated basing on the measurement of g, the insulin infusion and the CHO intake at the present time. In our work, we refer to the *UVa/Padova T1D* model. As previously described, this model's parameters are not unique but depend on the considered virtual patient. Rather than adopting its individualized form for each tested patient, we resort to the average one, i.e. referred to the average patient, whose parameters are precisely the mean of those of all the available virtual subjects. Even if this introduces a

[6] The effect of a control action is appreciable at the next sampling time, with respect to when it is computed and applied, i.e. when a new measurement is available.

certain degree of approximation, this is done for practical feasibility: indeed, the same model can be used in a real scenario as well, where the individual model of a real person is hard if not impossible to be known, instead.

In the following, we describe the implementation of the three MPCs we consider, starting from the singleMPC, passing through the dualMPC and concluding with the tripleMPC, which is the core objective of our project.

2.1. singleMPC

The single-hormone MPC acts on one variable only, denoted as $i(k)$, that is how much insulin the pump releases at each time k. This is a LMPC (Linear Model Predictive Control), since it is based on a linearized, and discretized, version of the metabolic system's model employed in the *UVa/Padova T1D* Simulator. The discretization is performed with a sampling time $T_s = 5$ min (the period the CGM sensor works with), while the linearization is made around the basal equilibrium point (of the average patient), obtained with basal insulin infusion ($i(k) = i_b(k)$) and no disturbance ($d(k) = 0$ mg). To do this, we resort to the *Model Linearizer App*, included in *Simulink®*. The resulting model, in state-space form, is the following:

$$\begin{cases} \bar{x}(k+1) = A\bar{x}(k) + B\bar{\imath}(k) + M\hat{d}(k) \\ \bar{g}(k) = C\bar{x}(k) \end{cases} \quad (1)$$

where:

- k is the time step;
- $\bar{x} \in R^{16\times 1}$ is the state;
- $\bar{g} \in R\left[\frac{\text{mg}}{\text{dl}}\right]$ is the difference between $g(k)$ and the basal glucose G_b of the patient;
- $\bar{\imath} \in R\left[\frac{\frac{\text{pmol}}{\text{min}}}{\text{kg}}\right]$ is the deviation of the insulin infusion $i(k)$ from the basal one of the patient, normalized by the body weight BW of the subject, i.e.

$$\bar{\imath}(k) = \frac{i(k) - i_b(k)}{BW}; \quad (2)$$

- $\hat{d} \in R_0^+$ [mg] is the announced meal's CHO consumption.
- $A \in R^{16\times 16}, B \in R^{16\times 1}, M \in R^{16\times 1}, C \in R^{1\times 16}$ are matrices.

The current state $\bar{x}(k)$ is unknown but it can be estimated via Kalman filter, basing on the current-time values of the CGM reading, of the insulin infusion and of the CHO intake. Further details are reported in section 2.4.

The MPC optimization problem explained above is solved by minimizing the following quadratic cost function, with respect to the sequence of insulin doses $\bar{\iota}(\cdot)$:

$$\tilde{J}\big(\bar{x}(k), k, \bar{\iota}(\cdot)\big) = \sum_{j=0}^{PH-1} \Big(\big(\bar{g}(k+j) - \overline{g_0}(k+j)\big)^2 + \tilde{r}\big(\bar{\iota}(k+j) - \overline{\iota_0}(k+j)\big)^2 \Big) + \|\bar{x}(k+PH)\|_P^2 \quad (3)$$

The first term in (3) is needed to penalize a deviation of $\bar{g}(k)$ from the desired reference $\overline{g_0}(k) = g_0(k) - G_b$, while the second one is introduced to discourage large control actions with respect with to a suitable reference $\overline{\iota_0}(k) = \frac{i_0(k) - i_b(k)}{BW}$. How much weight and thus importance the latter has with respect to the former is determined by the parameter $\tilde{r} \in R^+$: with a small $\tilde{r}$ the adherence of g to its reference is promoted, regardless of the amount of insulin i; conversely, the focus is on how much the computed insulin quantity is close to its reference, giving less importance to the quality of control. We suggest to refer to the appendix A.1, for a better understanding of the adopted notation.

The signal $\overline{\iota_0}(k)$ is obtained basing on the traditional manual therapy, adding the meal boluses i_{meal}(k) to the basal insulin:

$$i_0(k) = i_b(k) + i_{meal}(k),$$

therefore

$$\overline{\iota_0}(k) = \frac{i_{meal}(k)}{BW} \quad (4).$$

The signal $i_{meal}(k)$ is defined as in [24]:

$$i_{meal}(k) = \begin{cases} \dfrac{\hat{d}(k)}{CR} + \dfrac{g(k) - G_b}{CF} - IOB(k) & at\ meal\ times \\ 0 & otherwise \end{cases} \quad (5)$$

where CR and CF are patient-specific parameters and represent the carbohydrates-to-insulin ratio (i.e. how much grams of ingested CHO are covered by 1 U of insulin) and the correction factor (i.e. the glucose drop caused by 1 U of insulin), respectively. $IOB(k)$ stands for the insulin-on-board, i.e. the quantity of insulin that is still active at time k, and is computed as

reported in [5]. A further discussion about the meaning and the implementation of i_{meal} is present in the appendix A.2.

The third term in (3) $\|\bar{x}(k+PH)\|_P^2 = \bar{x}(k+PH)^T P \bar{x}(k+PH)$ is the terminal cost and is needed to take into account the system's response at time $k+PH$ as well. The state $\bar{x}$ is considered instead of the output $\bar{g}$ to promote stability. The weight P is computed by solving the Riccati equation:

$$P = A^T PA - (A^T PB)(rI + B^T PB)^{-1}(B^T PA) + qI \quad (6)$$

which has a unique non-negative solution and where I is the identity matrix and q and r are such that $\tilde{r} = \frac{r}{q}$.

In addition, the constraints on the minimal and maximal administrable dose of insulin (due to the actuator's physical limits):

$$0 \leq i(k) \leq i_{max}(k) \quad \forall k$$

are taken into account and become, after the same normalization i and i_0 undergo to:

$$\bar{\iota}_{min}(k) \leq \bar{\iota}(k) \leq \bar{\iota}_{max}(k) \quad \forall k \quad (7)$$

where $\bar{\iota}_{min}(k) = -\frac{i_b(k)}{BW}$ and $\bar{\iota}_{max}(k) = \frac{i_{max}(k) - i_b(k)}{BW}$.

The MPC optimal control problem can be summed up as following:

$$\min_{\substack{\bar{\iota}(\cdot) s.t. \\ \bar{\iota}_{min}(\cdot) \leq \bar{\iota}(\cdot) \leq \bar{\iota}_{max}(\cdot)}} \tilde{J}(\bar{x}(k), k, \bar{\iota}(\cdot)) \quad (8)$$

The MPC algorithm modulates the standard insulin reference $\bar{\iota_0}(k)$ at any time k, respecting the constraints. How the modulation is done depends on the trade-off it does between how much large the deviations of $\bar{g}$ and $\bar{\iota}$ from their own respective reference signals (i.e. the first two penalty terms in (3)) are. How that trade-off is solved is strongly determined by $\tilde{r}$, which has to be tuned specifically for each patient, due to the high inter-patient biovariability. This individualized tuning is discussed in section IV.

Finally, with the proper manipulations (reported in detail in appendix A.3), the problem previously described can be rewritten in a more compact matrix form and thus reconducted to a Quadratic Programming (QP) problem:

$$\min_{\substack{U \ s.t. \\ F_S U \leq f_S}} \frac{1}{2} U^T Q_S U + c_S^T U \quad (9)$$

where

$$U(k) = \begin{bmatrix} \bar{\iota}(k) \\ \vdots \\ \bar{\iota}(k + PH - 1) \end{bmatrix} \in R^{PH \times 1} \quad (10),$$

$$F_s = \begin{bmatrix} -I_{PH} \\ I_{PH} \end{bmatrix} \in R^{2PH \times PH}, \quad f_s(k) = \begin{bmatrix} -\bar{I}_{min}(k) \\ \bar{I}_{max}(k) \end{bmatrix} \in R^{2PH \times 1} \quad (11),$$

$$I_{PH} = \begin{bmatrix} 1 & 0 & \dots & 0 \\ 0 & \ddots & & \vdots \\ \vdots & & \ddots & 0 \\ 0 & \dots & 0 & 1 \end{bmatrix} \in R^{PH \times PH}$$

with

$$\bar{I}_{min}(k) = \begin{bmatrix} \bar{\iota}_{min}(k) \\ \vdots \\ \bar{\iota}_{min}(k) \end{bmatrix} \in R^{PH \times 1}, \quad \bar{I}_{max}(k) = \begin{bmatrix} \bar{\iota}_{max}(k) \\ \vdots \\ \bar{\iota}_{max}(k) \end{bmatrix} \in R^{PH \times 1}$$

and suitable matrix $Q_s \in R^{PH \times PH}$ and vector $c_s \in R^{PH \times 1}$, representing in matrix form the cost function (3).

2.2. dualMPC

The dualMPC proposed by Pavan et al. in [17] introduces a second control variable $c(k) \in R$, representing the suggested extra-CHO intakes; therefore, the model has to be modified as follows:

$$\begin{cases} \bar{x}(k+1) = A\bar{x}(k) + B\bar{\iota}(k) + M\hat{d}(k) + Mc(k) \\ \bar{g}(k) = C\bar{x}(k) \end{cases} \quad (12)$$

The new variable is defined as

$$c(k) = \gamma_1 c_1(k) + \gamma_2 c_2(k) \quad (13),$$

where $\gamma_1 = 1000 \frac{\text{mg}}{\text{min}}$ and $\gamma_2 = 2000 \frac{\text{mg}}{\text{min}}$, while $c_1, c_2 \in \{0,1\}$ are two Boolean support variables. As better discussed later, these variables will be bound not to be both active at the same time, i.e. to be mutually exclusive. In this way, $c(k)$ is quantized and can assume three values only, precisely 0, γ_1 or γ_2 [17].

An additional term is added to the cost function too, which becomes:

$$\tilde{J}\left(\bar{x}(k), k, \bar{\iota}(\cdot)\right) = \sum_{j=0}^{PH-1} \Big(\left(\bar{g}(k+j) - \overline{g_0}(k+j)\right)^2 + \tilde{r}\left(\bar{\iota}(k+j) - \overline{\iota_0}(k+j)\right)^2 + \tilde{s}(c_1(k+j)^2 + c_2(k+j)^2) \Big) + \|\bar{x}(k+PH)\|_P^2 \quad (14)$$

As a result, there is also a penalty on the ℓ_0-norm of the signal $c(\cdot)$, that is the number of its non-zero elements, in the prediction horizon (i.e. $c(k+j)$, for $j = 1, \dots, PH-1$). In other words, the number of CHO suggestions is penalized, independently from their amount [17]. There is a better explanation of what the ℓ_0-norm is in appendix A.1.

To promote sparsity in time of the CHO suggestions, in such a way to prevent frequent requests of patient intervention, a minimal distance Δ_c between two consecutive CHO intakes is imposed. This is obtained with the following constraint on the Boolean support variables:

$$\sum_{i=j}^{j+\Delta_c-1} (c_1(k+i) + c_2(k+i)) \leq 1 \quad \forall j = 0, \dots, PH - \Delta_c \quad (15)$$

that can be rewritten in the more compact matrix form

$$\tilde{F}_c C_{1,2}(k) \leq \tilde{f}_c \quad (16)$$

where

$$C_{1,2}(k) = [c_1(k), \dots, c_1(k+PH-1), c_2(k), \dots, c_2(k+PH-1)]^T \in R^{2PH\times 1},$$

$$\tilde{F}_c = \begin{bmatrix} \tilde{F}_{c_1} & \tilde{F}_{c_2} \end{bmatrix}, \quad \tilde{F}_{c_1} = \tilde{F}_{c_2} = \begin{cases} \overbrace{\begin{bmatrix} 1 & \dots & 1 \\ 0 & 1 & \dots \\ \vdots & & \ddots \\ \vdots & & \\ 0 & \dots & \dots \end{bmatrix}}^{\Delta_c} \overbrace{\begin{bmatrix} 0 & \dots & \dots & 0 \\ 1 & 0 & \dots & 0 \\ & \ddots & & \vdots \\ \ddots & & \ddots & 0 \\ 0 & 1 & \dots & 1 \end{bmatrix}}^{PH-\Delta_c} \in R^{(PH-\Delta_c+1)\times PH} & if\ PH > \Delta_c \\ [1 \quad \dots \quad 1] \in R^{1\times PH} & otherwise \end{cases},$$

$$\tilde{f}_c = \begin{cases} [1 \quad \dots \quad 1]^T \in R^{PH-\Delta_c+1} & if\ PH > \Delta_c \\ 1 & otherwise \end{cases}.$$

In this way, in every possible interval of length Δ_c within the prediction horizon, at most only one term between all the c_1's and c_2's in that period of time can be active. In particular, at each time within every interval the mutual exclusivity of c_1 and c_2 is imposed.

However, the above constraints do not fully ensure the sparsity, because they restrict only to the planned CHO suggestions at the current time k, while the CHO intakes suggested in the past, which are not included within the current prediction horizon, are not considered. As an

example, the optimal solution at time $k-1$ can include an extra-CHO at the beginning of the prediction horizon; that extra-CHO is consumed at the next step k, but it is not taken into account in the new optimization problem that is formulated at k. In addition, we similarly want to force a minimal distance Δ_m to the CHO suggestions from the last meal announcement [17], not to exacerbate the glycaemic rise. To achieve all this, another time-varying constraint is imposed:

$$c_1(k+i) + c_2(k+i) \leq c_{max}(k+i) \quad \forall i = 0, \dots, PH-1 \quad (17)$$

where c_{max} is a variable defined as

$$c_{max}(k+i) = \begin{cases} 0 & if\ k+i-k_{last}^{CHO} \leq \Delta_c \\ & or\ if\ k+i-k_{last}^{meal} \leq \Delta_m \\ 1 & otherwise \end{cases} \quad (18)$$

where k_{last}^{CHO} and k_{last}^{meal} are used to memorize the times of the last extra-CHO intake and the last meal, respectively.

If rewritten in matrix form, the above constraint is:

$$\tilde{F}_{max}^{c} C_{1,2}(k) \leq C_{max}(k) \quad (19)$$

with

$$\tilde{F}_{max}^{c} = [I_{PH} \quad I_{PH}] \in R^{PH \times 2PH}, \quad C_{max}(k) = [c_{max}(k) \quad \dots \quad c_{max}(k+PH-1)]^T \in R^{PH \times 1}.$$

To limit the number of CHO suggestions the algorithm can give in a day to an upper bound n_{max}, another time-varying constraint is introduced, that is

$$\sum_{i=0}^{PH-1} (c_1(k+i) + c_2(k+i)) \leq n_{res}(k) \quad (20)$$

where $n_{res}(k)$ is the residual number of extra-CHO intakes that can be given in a day; it is decreased of one unit every time a CHO suggestion is given and it is reset to n_{max} every day at $06{:}00$ AM.

Finally, the introduction of "do-not-disturb" zones, namely time intervals where no CHO suggestions can be given, is requested, in order to avoid the intervention of the patient in predefined periods of the day, when it is expected to be problematic if not impossible. To achieve this, it is sufficient to force $n_{res}(k)$ to be zero in these periods. In our work, we set up a "do-not-disturb" zone during every night, from $00{:}00$ to $06{:}00$ AM.

The above constraint can be translated in matrix form as follows:

$$[\overbrace{1 \quad \dots \quad 1}^{2PH}]C_{1,2}(k) \leq n_{res}(k).$$

The optimization problem reported above can be formulated in a more compact form as a Mixed Integer Quadratic Programming (MIQP) problem (not just as a QP due to the presence of the Boolean support variables), as explained in appendix A.3 as well:

$$\min_{\substack{U \ s.t. \\ F_d U \leq f_d \\ U_{PH+1,\dots,3PH} \in \{0,1\}}} \frac{1}{2} U^T Q_d U + c_d^T U \quad (21)$$

following a procedure analogous to that used to obtain the formula (9), redefining $U(k)$ as

$$U(k) = \begin{bmatrix} \bar{\iota}(k) \\ \vdots \\ \bar{\iota}(k + PH - 1) \\ C_{1,2}(k) \end{bmatrix} \in R^{3PH}, \quad (22)$$

with

$$F_d = \begin{bmatrix} & & -I_{3PH} & & & \\ & & & 0 & \cdots & 0 \\ & I_{PH} & & \vdots & \ddots & \vdots \\ & & & 0 & \cdots & 0 \\ 0 & \dots & 0 & \tilde{F}_{max}^c & & \\ \vdots & \ddots & \vdots & \tilde{F}_c & & \\ 0 & \dots & 0 & 1 & \dots & 1 \end{bmatrix} \in R^{(6PH - \Delta_c + 2) \times 3PH}, \quad f_d(k) = \begin{bmatrix} -U_{min}^d(k) \\ U_{max}^d(k) \\ \tilde{f}_c \\ n_{res}(k) \end{bmatrix} \in R^{6PH - \Delta_c + 2 \times 1} \quad (23)$$

$$I_{3PH} = \begin{bmatrix} 1 & 0 & \dots & 0 \\ 0 & \ddots & & \vdots \\ \vdots & & \ddots & 0 \\ 0 & \dots & 0 & 1 \end{bmatrix} \in R^{3PH \times 3PH},$$

$$U_{min}^d(k) = \begin{bmatrix} I_{min}(k) \\ 0 \\ \vdots \\ 0 \end{bmatrix} \in R^{3PH \times 1}, \quad U_{max}^d(k) = \begin{bmatrix} I_{max}(k) \\ C_{max}(k) \end{bmatrix} \in R^{2PH \times 1}$$

and suitable matrix $Q_d \in R^{PH \times PH}$ and vector $c_d \in R^{PH \times 1}$.

2.3. tripleMPC

The core objective of our project is to introduce in AP the capability to administer corrective insulin boluses (as well as CHO suggestions), thus implementing the so-called tripleMPC. As anticipated in the introduction, this option has already been explored, however resorting to mere heuristic methods or a separate independent module [18-19]. The characteristic of tripleMPC

which distinguish it from these mentioned approaches, and which makes it innovative is that the corrective boluses are included with a real additional control variable. In this way they are proactively planned as well, in synergy with basal insulin modulation and the planning of the CHO suggestions. We choose to represent the boluses with the continuous variable $b(k) \in R_0^+$.

A Boolean support variable $z(k) \in \{0,1\}$ is needed as well, to model the ability of the algorithm to choose whether to administer a bolus or not, and so to have that $b(k) \neq 0$ only if $z(k)$ is active (otherwise b would be continuously modulated, as well as the basal insulin i). This is achieved imposing the following time-variant lower and upper bounds on $b(k)$:

$$m \cdot z(k) \leq b(k) \leq M \cdot z(k) \quad \forall k \quad (24)$$

where $m \in R_0^+$ and $M \in R^+$ are constants, with $m < M$; in this way, when $z(k) = 0$, $b(k)$ is forced to be null, vice versa, when $z(k)$ is active, $b(k)$ is free to assume any value ranging from m to M. In our work we set $m = \frac{50}{CF}\ \frac{\text{U}}{\text{min}}$, i.e. the (individualized) minimum quantity of insulin that is expected to lead to a glucose drop of $50\ \frac{\text{mg}}{\text{dl}}$, and $M = 100\ \frac{\text{U}}{\text{h}} \cong 1.67\ \frac{\text{U}}{\text{min}}$. Notice that $m \neq 0$: this is to avoid the otherwise possible delivering of small and so not impactful boluses, which would hardly be practically useful.

These bounds can be rewritten using the matrix notation, as:

$$\begin{bmatrix} -I_{PH} & m \cdot I_{PH} \\ I_{PH} & -M \cdot I_{PH} \end{bmatrix} \begin{bmatrix} B(k) \\ Z(k) \end{bmatrix} \leq [\overbrace{0 \quad \dots \quad 0}^{PH}]^T \quad (25)$$

where

$$B(k) = [b(k), \dots, b(k + PH - 1)]^T \in R^{PH \times 1}, \quad Z(k) = [z(k), \dots, z(k + PH - 1)]^T \in R^{PH \times 1}.$$

The model must be modified and becomes:

$$\begin{cases} \bar{x}(k+1) = A\bar{x}(k) + B\bar{\imath}(k) + M\hat{d}(k) + Mc(k) + Bb(k) \\ \bar{g}(k) = C\bar{x}(k) \end{cases} \quad (26)$$

where $c(k)$ is defined as in (13), but now with γ_1 and γ_2 increased to 3000 and 4000 $\frac{\text{mg}}{\text{min}}$, respectively, since with the extra boluses the total quantity of administered insulin is more consistent and the expected risk of major hypoglycaemic events must be prevented.

The cost function is also extended, as follows:

$$\tilde{J}\left(\bar{x}(k), k, \bar{\iota}(\cdot)\right) = \sum_{j=0}^{PH-1} \Big(\left(\bar{g}(k+j) - \overline{g_0}(k+j)\right)^2 + \tilde{r}\left(\bar{\iota}(k+j) - \overline{\iota_0}(k+j)\right)^2 + \tilde{s}(c_1(k+j)^2 + c_2(k+j)^2) + \widetilde{w}_1 b(k+j)^2 + \widetilde{w}_2 z(k+j)^2 \Big) + \|\bar{x}(k+PH)\|_P^2 \quad (27)$$

De facto, the signal $z(\cdot)$ takes into account the number of administered extra-boluses. Therefore, in this way both the quantity and the number of corrective boluses are penalized, as well. The weight $\widetilde{w}_1$ should be relatively small, since the quantity penalization has to be intended as a way only to prevent the algorithm to deliver excessively large boluses. The penalization of the number, instead, is introduced to promote the boluses' delivering only when actually needed.

The support variable $z(k)$ is necessary to promote the sparsity in time of the corrective boluses, as well. This can be achieved by imposing on it constraints similar to (15) and (17), i.e.:

$$\sum_{i=j}^{j+\Delta_b-1} (z(k+i)) \leq 1 \quad \forall j = 0, \dots, PH - \Delta_b \quad (28)$$

with Δ_b the minimal distance between two consecutive corrective boluses that we want, and

$$z(k+i) \leq z_{max}(k+i) \quad \forall i = 0, \dots, PH-1,$$

with

$$z_{max}(k+i) = 0 \quad if\ k + i - k_{last}^{bolus} \leq \Delta_b,$$

where k_{last}^{bolus} is the time of the last corrective bolus administration.

These can be rewritten in matrix form, respectively as:

$$\tilde{F}_b Z(k) \leq \tilde{f}_b \quad (29)$$

with

$$\tilde{F}_b = \begin{cases} \begin{bmatrix} \overbrace{1 & \dots & 1}^{\Delta_b} & \overbrace{0 & \dots & \dots & 0}^{PH-\Delta_b} \\ 0 & 1 & \dots & 1 & 0 & \dots & 0 \\ \vdots & & \ddots & & \ddots & & \vdots \\ \vdots & & & \ddots & & \ddots & 0 \\ 0 & \dots & \dots & 0 & 1 & \dots & 1 \end{bmatrix} \in R^{(PH-\Delta_b+1)\times PH} & if\ PH > \Delta_b, \\ [1 \quad \dots \quad 1] \in R^{1\times PH} & otherwise \end{cases}$$

$$\tilde{f}_b = \begin{cases} [1 \quad \dots \quad 1]^T \in R^{PH-\Delta_b+1} & if\ PH > \Delta_b \\ 1 & otherwise \end{cases}$$

and

$$I_{PH} Z(k) \leq Z_{max}(k), \quad (30)$$

with

$$Z_{max}(k) = [z_{max}(k) \quad \dots \quad z_{max}(k+PH-1)]^T \in R^{PH\times 1}.$$

In addition, we want to introduce a minimal distance Δ_{bc} between the suggested CHO intakes and the extra boluses, to avoid the simultaneous use of these aggressive and antagonistic control actions; this is obtained with the following constraint:

$$\sum_{i=j}^{j+\Delta_{bc}-1} (c_1(k+i) + c_2(k+i) + z(k+i)) \leq 1 \quad \forall j = 0, \dots, PH - \Delta_{bc} \quad (31)$$

that can be rewritten as

$$[\tilde{F}_{bc} \quad \tilde{F}_{bc} \quad \tilde{F}_{bc}] \begin{bmatrix} C_{1,2}(k) \\ B(k) \end{bmatrix} \leq \tilde{f}_{bc} \quad (32)$$

with

$$\tilde{F}_{bc} = \begin{cases} \overbrace{\begin{bmatrix} 1 & \dots & 1 \\ 0 & 1 & \dots \\ \vdots & & \ddots \\ \vdots & & \\ 0 & \dots & \dots \end{bmatrix}}^{\Delta_{bc}} \overbrace{\begin{bmatrix} 0 & \dots & \dots & 0 \\ 1 & 0 & \dots & 0 \\ & \ddots & & \vdots \\ \ddots & & \ddots & 0 \\ 0 & 1 & \dots & 1 \end{bmatrix}}^{PH-\Delta_{bc}} \in R^{(PH-\Delta_{bc}+1)\times PH} & if\ PH > \Delta_{bc}, \\ [1 \quad \dots \quad 1] \in R^{1\times PH} & otherwise \end{cases}$$

$$\tilde{f}_{bc} = \begin{cases} [1 \quad \dots \quad 1]^T \in R^{PH-\Delta_{bc}+1} & if\ PH > \Delta_{bc} \\ 1 & otherwise \end{cases}$$

and adding that

$$c_{max}(k+i) = 0 \quad if\ k+i-k_{last}^{bolus} \leq \Delta_{bc} \text{ and } z_{max}(k+i) = 0 \quad if\ k+i-k_{last}^{CHO} \leq \Delta_{bc}.$$

A minimal distance Δ_m^b from a meal to a corrective bolus is needed as well, since a further bolus intake after a meal is likely to lead to hypoglycaemia. This is due to the delay in insulin action and therefore to the fact that the bolus can take effect when the glycaemic level has already dropped. Moreover, typically it can be hard for our MPC to foresee accurately the long-term effect of a bolus in such a situation. This is because the linearized model we adopt for our MPC

is limited exactly when near hypoglycaemia and when referring to a relatively far future time; therefore, the MPC's model-based predictions are less accurate in these conditions. This can be included imposing that

$$z_{max}(k+i) = 0 \quad if\ k+i-k_{last}^{meal} \leq \Delta_m^b.$$

Lastly, since we want to include the use of emergency hypotreatments as well, we impose that

$$c_{max}(k+i) = 0 \quad if\ k+i-k_{last}^{eHT} \leq \Delta_c$$

where k_{last}^{eHT} is the time of the last emergency hypotreament, in order to have the minimal distance Δ_c also between the emergency hypotreatments and the planned ones[7].

Overall, c_{max} (for the tripleMPC) and z_{max} are respectively defined as

$$c_{max}(k+i) = \begin{cases} & if\ k+i-k_{last}^{CHO} \leq \Delta_c, \\ 0 & if\ k+i-k_{last}^{meal} \leq \Delta_m, \\ & if\ k+i-k_{last}^{bolus} \leq \Delta_{bc} \\ & or\ if\ k+i-k_{last}^{eHT} \leq \Delta_c \\ 1 & otherwise \end{cases} \quad (33)$$

$$z_{max}(k+i) = \begin{cases} & if\ k+i-k_{last}^{bolus} \leq \Delta_b, \\ 0 & if\ k+i-k_{last}^{meal} \leq \Delta_m^b \\ & or\ if\ k+i-k_{last}^{CHO} \leq \Delta_{bc} \\ 1 & otherwise \end{cases}$$

Finally, as similarly as for the dualMPC and as discussed in appendix A.3, we can reconduct to the MIQP formulation of the problem

$$\min_{\substack{U\ s.t. \\ F_t U \leq f_t \\ U_{PH+1,\dots,3PH} \in \{0,1\} \\ 4PH+1,\dots,5PH}} \quad \frac{1}{2} U^T Q_t U + c_t^T U \quad (34)$$

redefining $U(k)$ as

$$U(k) = \begin{bmatrix} \bar{\imath}(k) \\ \vdots \\ \bar{\imath}(k+PH-1) \\ C_{1,2}(k) \\ B(k) \\ Z(k) \end{bmatrix} \in R^{5PH \times 1}, \quad (35)$$

[7] To fully accomplish this, in true it is necessary also to work on the separate module that manages the emergency hypotreatments, which we could not do due to our timetable. For the same reason, we could not include the last modification regarding c_{max} for the dualMPC too, since this would have meant redoing all the relative tests, that had already been done when we figured out all this is needed.

with

$$F_t = \begin{bmatrix} -F_{min}^t \\ F_{max}^t \\ \tilde{F} \end{bmatrix} \in R^{(12PH-\Delta_c-\Delta_b-\Delta_{bc}+4)\times 5PH},$$

$$f_t(k) = \begin{bmatrix} -U_{min}^t(k) \\ U_{max}^t(k) \\ \tilde{f}_c \\ n_{res}(k) \\ \tilde{f}_b \\ \tilde{f}_{bc} \end{bmatrix} \in R^{12PH-\Delta_c-\Delta_b-\Delta_{bc}+4\times 1} \tag{36}$$

$$F_{min}^t = \begin{bmatrix} I_{PH} & 0 & \dots & \dots & \dots & 0 \\ 0 & I_{PH} & \ddots & & & \vdots \\ \vdots & \ddots & I_{PH} & 0 & \dots & 0 \\ \vdots & & \ddots & I_{PH} & -m \cdot I_{PH} & \\ 0 & \dots & \dots & 0 & I_{PH} & \end{bmatrix} \in R^{5PH\times 5PH},$$

$$F_{max}^t = \begin{bmatrix} & & & 0 & \cdots & 0 & & & & 0 & \cdots & 0 \\ & I_{PH} & & \vdots & \ddots & \vdots & & I_{PH} & & \vdots & \ddots & \vdots \\ & & & 0 & \cdots & 0 & & & & 0 & \cdots & 0 \\ 0 & \cdots & 0 & & & & 0 & \cdots & \cdots & \cdots & \cdots & 0 \\ \vdots & \ddots & \vdots & & \tilde{F}_{max}^c & & \vdots & & \ddots & & \ddots & \vdots \\ 0 & \cdots & 0 & & & & 0 & \cdots & \cdots & \cdots & \cdots & 0 \\ 0 & \cdots & \cdots & \cdots & \cdots & 0 & & & & & & \\ \vdots & & \ddots & & \ddots & \vdots & & I_{PH} & & & -M \cdot I_{PH} & \\ 0 & \cdots & \cdots & \cdots & \cdots & 0 & & & & & & \\ 0 & \cdots & \cdots & \cdots & \cdots & \cdots & \cdots & \cdots & 0 & & & \\ \vdots & & \ddots & & \ddots & & \ddots & & \vdots & & I_{PH} & \\ 0 & \cdots & \cdots & \cdots & \cdots & \cdots & \cdots & \cdots & 0 & & & \end{bmatrix} \in R^{4PH\times 5PH},$$

$$\tilde{F} = \begin{bmatrix} 0 & \dots & 0 & & & & 0 & \dots & \dots & \dots & \dots & 0 \\ \vdots & \ddots & \vdots & & \tilde{F}_c & & \vdots & \ddots & & \ddots & & \vdots \\ \vdots & \ddots & \vdots & & & & \vdots & & \ddots & & \ddots & \vdots \\ 0 & \dots & 0 & 1 & \dots & 1 & 0 & \dots & \dots & \dots & \dots & 0 \\ 0 & \dots & \dots & \dots & \dots & \dots & \dots & \dots & 0 & & & \\ \vdots & & \ddots & & \ddots & & \ddots & & \vdots & & \tilde{F}_b & \\ 0 & \dots & \dots & \dots & \dots & \dots & \dots & \dots & 0 & & & \\ 0 & \dots & 0 & & & & 0 & \dots & 0 & & & \\ \vdots & & \vdots & \tilde{F}_{bc} & & \tilde{F}_{bc} & \vdots & & \vdots & & \tilde{F}_{bc} & \\ 0 & \dots & 0 & & & & 0 & \cdots & 0 & & & \end{bmatrix} \in R^{(3PH-\Delta_c-\Delta_b-\Delta_{bc}+4)\times 5PH},$$

$$U_{min}^t(k) = \begin{bmatrix} I_{min}(k) \\ 0 \\ \vdots \\ 0 \end{bmatrix} \in R^{5PH\times 1}, \quad U_{max}^t(k) = \begin{bmatrix} I_{max}(k) \\ C_{max}(k) \\ 0 \\ \vdots \\ 0 \\ Z_{max}(k) \end{bmatrix} \in R^{4PH\times 1}$$

and suitable matrix $Q_t \in R^{PH \times PH}$ and vector $c_t \in R^{PH \times 1}$.

Notice that now the upper bound for the administrable dose of insulin is imposed on the sum of i and b, i.e.

$$\bar{\imath}(k) + b(k) \leq \bar{\imath}_{max}(k) \quad \forall k. \quad (37)$$

Finally, we specify that the optimization problem (9) was solved by using *Matlab®* and, regarding (21) and (34), also resorting to *ILOG CPLEX Optimization Studio®* (v. 12.9) [25].

2.4. State estimate

To estimate the state $\bar{x}$, we adopt a Kalman filter (KF). Starting from the assumptions that there is a model-plant mismatch and that the sensor cannot be perfectly accurate, the model error $v_x(k)$ and the measurement noise $v_y(k)$ are introduced in the model[8], thus switching to a stochastic description:

$$\begin{cases} \bar{x}(k+1) = A\bar{x}(k) + B\bar{\imath}(k) + M\hat{d}(k) + v_x(k) \\ \bar{g}(k) = C\bar{x}(k) + v_y(k) \end{cases} \quad (38)$$

with $[v_x, v_y]$ white Gaussian noises, independent, with zero mean and covariance matrix

$$Var\begin{bmatrix} v_x \\ v_y \end{bmatrix} = \begin{bmatrix} Q_x & S \\ S' & R_y \end{bmatrix} \in R^{17 \times 17}.$$

For simplicity, we assume that $S = 0$ and so that they are also uncorrelated. We set $R_y = 9.1692 \frac{\text{mg}^2}{\text{dl}^2}$ and the non-null elements $q_1, \dots, q_{16}$ of the diagonal matrix Q_x to the values reported in Table I, by referring to [13][9].

The KF is initialized with $\bar{x}(0) = 0$; then the state estimation, at a certain time k, is performed by following an iterative strategy made of two steps:

1) the KF predicts the state for the current time $\hat{x}(k|k-1)$, basing on the state estimate $\hat{x}(k-1|k-1)$ from the previous iteration (at time $k-1$) and assuming that $v_x(k) = E[v_x(k)] = 0$, i.e.:

[8] Here we consider the basic model the singleMPC refers to, but the reported reasoning can be straightforwardly extended to the other models.

[9] With respect to [13], in the version of the *UVa/Padova T1D* Simulator we use, there are 3 additional states. Therefore, in true we set $q_1, \dots, q_{13}$ to the values reported in [13], while we established the additional terms $q_{14}, \dots, q_{16}$ by trial and error.

$$\hat{x}(k|k-1) = A\hat{x}(k-1|k-1) + Bi(k) + M\hat{d}(k); \quad (39)$$

2) when the measurement for the current time $g(k)$ becomes available, it is exploited to update the previously predicted state:

$$\hat{x}(k|k) = \hat{x}(k|k-1) + L\big(\bar{g}(k) - C\hat{x}(k|k-1)\big). \quad (40)$$

L is the (constant) observer gain and it is defined as:

$$L = PC^T(CPC^T + R_y)^{-1} \quad (41)$$

with P the positive-definite matrix which is the unique solution to the Riccati equation

$$P = APA^T + Q_x - APC^T\big(CPC^T - R_y\big)^{-1}CPA^T \quad (42)$$

that can be computed offline, as well as L.

Table I. Diagonal elements of the matrix Q_x.

Element	Value [%]	Measurement unit
q_1, q_2, q_3	0.1	mg^2
q_4, q_5	10	$\left(\frac{\mathrm{mg}}{\mathrm{kg}}\right)^2$
q_6, q_7, q_8	0.1	$\left(\frac{\mathrm{pmol}}{\mathrm{l}}\right)^2$
$q_9, q_{10}, q_{11}, q_{12}$	0.1	$\left(\frac{\mathrm{pmol}}{\mathrm{kg}}\right)^2$
q_{13}	10	$\left(\frac{\mathrm{mg}}{\mathrm{dl}}\right)^2$
q_{14}, q_{15}, q_{16}	0.1	$\left(\frac{\mathrm{pmol}}{\mathrm{l}}\right)^2$

III. Experimental set-up

To tune and validate the algorithms previously described, we employed the *UVa/Padova T1D Simulator*®, an accurate model of a T1D patient's metabolism consisting in 16 nonlinear differential state-update equations (plus the static output equations), containing about 35 parameters. The model parameters are not unique; conversely, the simulator is coupled with a bunch of 100 virtual patients, i.e. different realizations of the parameters' set, sampled from a probability distribution inferred from clinical data and respecting the real inter-subject variability [20]. In 2008, it was accepted by the U.S. FDA (Food and Drug Administration) as a substitute of animal trials for preclinical testing of T1D therapies, thus representing a less expensive, more affordable and ethical option. In this work we adopt a subsequently updated version of this simulator (v. S2013), which was approved by the FDA as well in 2017, including several additional features: a model of the "dawn-phenomenon"[10], time-varying model parameters and suboptimal patients' therapy parameters [20]. These are optional features and, if enabled, significantly increase the realism of the simulation scenario.

The *UVa/Padova T1D* model is connected with a simulator of the functioning of a real CGM sensor, affected by white noise, and of course a module where the control algorithm is implemented, thus reproducing the logic architecture of the AP as well. The measurement error is also an optional property.

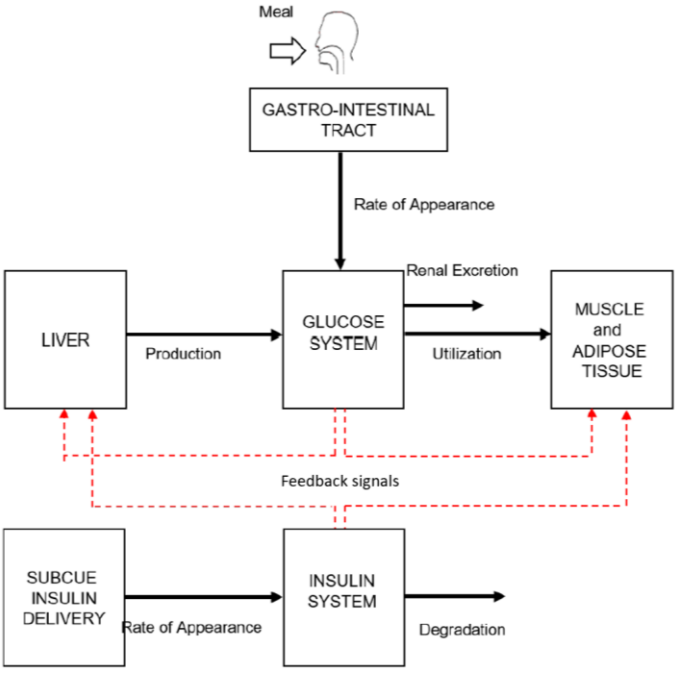

Figure 2. A schema of the *UVa/Padova T1D* metabolic model.

[10] The glycaemic rise that is typically found for T1D patients in the early morning.

The simulations of the functioning of the considered algorithms that we made last three days, starting from $00:00$ AM, each one including the consumption of three meals, which are announced by the patient to the system. The times of occurrence and the amount of CHOs of the meals vary between subjects and are sampled from uniform distributions, whose values accord to the range of the data in [26] and are reported in Table II. The meal announcements, together with the carb-counting error[11] (CCE) that is committed by the subject and affects the meal's CHO amount reported to the system, are simulated by a patient decisions' model [22], which is integrated with the *UVa/Padova T1D* simulator as well. It models also the generation mechanism of emergency hypotreatments (eHT), which are just triggered when the measured glycaemia drops below hypoglycaemia threshold levels; therefore, we will distinguish them from the planned ones (pHT), proposed by the dual- and the tripleMPC. The CCE and the eHT can be optionally included in the scenario, as well. More details on how the CCE is modelled and on the eHT generation mechanism can be found in [22] or in appendix A.4.

Table II. Ranges of the possible CHO amount and time of consumption of each meal.

Meal	CHO amount [g]	Time of consumption
Breakfast	$[19-97]$	$[06:30\ \text{AM}-08:00\ \text{AM}]$
Lunch	$[31-124]$	$[11:30\ \text{AM}-01:00\ \text{PM}]$
Dinner	$[28-140]$	$[06:00\ \text{PM}-08:30\ \text{PM}]$

The simulation scenario we choose is relatively realistic and in particular it can be set up enabling the "dawn-phenomenon", the time variability of the insulin sensitivity, the CGM sensor noise, the CCE and the eHT, and setting suboptimal values of CR and $i_b(k)$.

The described scenario is appropriate to test the performances of the single- and the dualMPC, but it is not expected to be the most appropriate to evaluate the actual potential of the tripleMPC; indeed, since we impose that the corrective boluses cannot be administered after a meal, until a period of time equal (at least) to Δ_m^b has elapsed, in general there is no other occasion in which the blood glucose rises so high that they become necessary. For this reason, an extra robustness test is performed, introducing in the previous simulation scenario, during the night and thus far from any meal, an unexplained hyperglycaemic event, which is more persistent and so more challenging with respect to post-prandial hyperglycaemia, and which is expected not to be addressable only modulating the basal insulin, as for the meals. This is achieved by adding an unannounced and prolonged CHO assumption. In detail, we introduce in each day an extra CHO

[11] The random error that can be committed by the patient estimating the CHO amount of a meal to be announced.

intake of 25 g from 00:00 to 00:30 AM, plus another one of 20 g from 00:30 to 05:00 AM, both with constant rate of assumption. In order to do a fair comparison between the three algorithms, this test is repeated for the other two MPCs as well. The introduction of such a disturbing factor, even if its generation mechanism is not properly realistic, makes sense, exactly because in a real scenario the hyperglycaemias are tipically more persistent, and do not occur only at mealtimes (as in the previous simulation scenario), because there may be other sources of hyperglycaemias (e.g., stress) apart from meals, in the rest of the day.

To evaluate the performances of the three versions of MPC, we adopt the standard metrics according to [27-28]. These include the time-in range (TIR), i.e. between 70 and 180 $\frac{\text{mg}}{\text{dl}}$, the time-below-range ($TBR$), i.e. below 70 $\frac{\text{mg}}{\text{dl}}$, the time-above-range ($TAR$), i.e. above 180 $\frac{\text{mg}}{\text{dl}}$, the time-in-deep-hypoglycaemia (TDh), i.e. below 55 $\frac{\text{mg}}{\text{dl}}$, the time-in-deep-hyperglycaemia (TDH), i.e. above 250 $\frac{\text{mg}}{\text{dl}}$, all in percentage. The mean μ_{CGM} and the standard deviation σ_{CGM} of the CGM signal are considered too. Moreover, we include the area-under-the-curve in hypoglycaemia (AUC_h), defined as the area between the glucose signal $g(k)$ and the hypoglycaemic threshold $BG_h = 70$ $\frac{\text{mg}}{\text{dl}}$, i.e.

$$AUC_h = \sum_{k=1}^{N} (\max(BG_h - g(k), 0))T_s \quad (43)$$

where N is the number of simulated CGM measurements, and, similarly, the area-under-the-curve in hyperglycaemia (AUC_H), i.e.

$$AUC_H = \sum_{k=1}^{N} (\max(g(k) - BG_H, 0))T_s \quad (44)$$

with the hyperglycaemic threshold $BG_H = 180$ $\frac{\text{mg}}{\text{dl}}$. In addition, we evaluate the daily average number n_{HT} and amount q_{HT} of ingested hypotreatments' CHO, which are both split between emergency and planned, for the dual- and the tripleMPC. The daily average number n_{bol} and amount q_{bol} of the administered extra boluses is taken into account as well, for the tripleMPC. Moreover, we consider also the metric TDI, that is the total-daily-insulin that the patient assumes on average. For the metrics with a Gaussian distribution, we report the population mean and standard deviation, while for the others the median and the interquartile range.

To compare the performances of the algorithms and particularly to evaluate the statistical significance of possible improvements regarding the metrics obtained with the tripleMPC, with

respect to the single- and the dualMPC, we resort to a paired-sample *t*-test, if the population of the considered metric has a Gaussian distribution, or a Wilcoxon signed rank test, otherwise. The normality of each distribution is evaluated by means of a Lilliefors test and the significance level is set to 5%, for all the three tests.

IV. Algorithms tuning

How much aggressively each algorithm acts on each control variable depends on the weights $\tilde{r}, \tilde{s}$ and the couple $\widetilde{w}_1$, $\widetilde{w}_2$, related to the inputs $i(k), c(k)$, and $b(k)$, respectively. Due to the high inter-subject variability concerning the metabolism and particularly the sensitivity to insulin and carbohydrates, it is hard to find fixed values for these hyperparameters that are appropriate for every patient; therefore, these parameters have to be individually optimized. All the other hyperparameters can be fixed instead; the values we used for these parameters are reported in Table III.

Table III. Fixed hyperparameters' values, for each algorithm.

Parameter	singleMPC	dualMPC	tripleMPC	Measurement unit
PH	12	12	24	-
$\bar{\iota}_{min}(k)$	$-\frac{i_b(k)}{BW}$	$-\frac{i_b(k)}{BW}$	$-\frac{i_b(k)}{BW}$	$\frac{\text{pmol}}{\frac{\text{min}}{\text{kg}}}$
$\bar{\iota}_{max}(k)$	$\frac{10^4 - i_b(k)}{BW}$	$\frac{10^4 - i_b(k)}{BW}$	$\frac{10^4 - i_b(k)}{BW}$	$\frac{\text{pmol}}{\frac{\text{min}}{\text{kg}}}$
γ_1	-	10^3	$3 \cdot 10^3$	$\frac{\text{mg}}{\text{min}}$
γ_2	-	$2 \cdot 10^3$	$4 \cdot 10^3$	$\frac{\text{mg}}{\text{min}}$
Δ_c	-	90	120	min
Δ_m	-	45	60	min
n_{max}	-	20	20	-
m	-	-	$\frac{3 \cdot 10^5}{\frac{CF}{BW}}$	$\frac{\text{pmol}}{\frac{\text{min}}{\text{kg}}}$
M	-	-	$\frac{10^4}{BW}$	$\frac{\text{pmol}}{\frac{\text{min}}{\text{kg}}}$
Δ_b	-	-	60	min
Δ_m^b	-	-	90	min
Δ_{bc}	-	-	90	min

The strategy for hyperparameters individualization we consider consists in testing several admissible points in the hyperparameters space and choosing the one associated to the best performances, according to a suitable cost function. This can be done in silico, but unfortunately

not in real patients, since dangerous BG levels could be reached in some tests. Hence, the solution we adopt is to train regression laws in silico, to be used to compute the personalized optimal hyperparameters also for real subjects, starting from patients' accessible parameters like CR or the body weight BW. Briefly, we proceed by following these three steps:

1) the 100 available virtual subjects are split in a training and a testing set, including 50 patients each, randomly sampled;
2) the optimal hyperparameters are retrieved for the subjects belonging to the training set and then used to infer the regression models;
3) the regression laws are used to compute suboptimal hyperparameters for the testing set.

These are repeated also in the simulation scenario for the robustness test (i.e. with the introduction of persistent hyperglycaemia).

More in detail, the cost function we use to evaluate the control performance and to be minimized in order to retrieve the optimal hyperparameters choice, for the training set, is a modified version of the Weighted Area Outside Target Range (wAOTR), defined as:

$$wAOTR = \alpha AUC_h + \beta AUC_H + \lambda q_{HT} \quad (45)$$

where α, β and λ are different weights assigned respectively to hypoglycaemia, hyperglycaemia and the total quantity in grams of the ingested extra-CHOs, both emergency and planned; the values we set them to are $\alpha = 1e3 \ \frac{\text{dl}}{\text{mg·min}}$, $\beta = 35 \ \frac{\text{dl}}{\text{mg·min}}$ and $\lambda = 5e3 \ \text{g}^{-1}$.

Table IV. Ranges for the Bayesian search of the individualized hyperparameters.

Parameter	singleMPC	dualMPC	tripleMPC	Measurement unit
$\tilde{r}$	$[10 - 10^7]$	$[1 - 10^6]$	$[1 - 10^6]$	$\left(\frac{\frac{\text{kg}}{\text{min}}}{\text{pmol}}\right)^2$
$\tilde{s}$	-	$[10 - 10^8]$	$[1 - 10^5]$	-
$\widetilde{w}_1$	-	-	$[10^{-3} - 1e2]$	$\left(\frac{\frac{\text{kg}}{\text{min}}}{\text{pmol}}\right)^2$
$\widetilde{w}_2$	-	-	$[1 - 10^4]$	-

Once the cost function is defined, the hyperparameter optimization is performed on the training set via Bayesian search [29]. In our work, we initialize the algorithm with N_r random points, then the objective function is evaluated N_e times, with $N_r = 20$ and $N_e = 60$ for the single-

and the dualMPC, while $N_r = 30$ and $N_e = 70$ for the tripleMPC. The ranges of values considered for $\tilde{r}, \tilde{s}, \widetilde{w}_1$ and $\widetilde{w}_2$ in which to search are indicated in Table III.

Finally, the achieved optimal hyperparameters are used to retrieve the regression laws we look for, via least square regression. Let us consider the p-th patient of the training set, with $p = 1, \dots, 50$, and let us denote, for the p-th subject, the optimal $\tilde{r}$ for the singleMPC with $\tilde{r}_s(p)$, the optimal $\tilde{r}$ and $\tilde{s}$ for the dualMPC with $\tilde{r}_d(p)$ and $\tilde{s}_d(p)$ and the optimal $\tilde{r}$, $\tilde{s}$, $\widetilde{w}_1$, $\widetilde{w}_2$ for the tripleMPC with $\tilde{r}_t(p)$, $\tilde{s}_t(p)$, $\widetilde{w}_1(p)$, $\widetilde{w}_2(p)$. We assume a log-linear regression model, that is:

$$\log(h(p)) = \varphi_h(p)\theta_h + \epsilon_h(p) \quad (46)$$

where $h \in \{\tilde{r}_s, \tilde{r}_d, \tilde{s}_d, \tilde{r}_t, \tilde{s}_t, \widetilde{w}_1, \widetilde{w}_2\}$ is one of the hyperparameters. $\varphi_h(p) \in R^{1 \times N_{reg}}$ is a vector containing N_{reg} regressors in patient p, i.e. a proper subset of patient's accessible parameters. This subset depends on which hyperparameter is considered and is selected from an initial pool of possible accessible parameters, which is $\left\{BW, CR_{avg}, CF, i_{b_{avg}}\right\}$ for the regression of $\tilde{r}_s, \tilde{r}_d, \tilde{r}_t, \tilde{s}_d, \tilde{s}_t$, and $\left\{Age, BW, CR_{avg}, CF, CL, i_{b_{avg}}, G_b, TDI\right\}$ for the two remaining hyperparameters, where CR_{avg} and $i_{b_{avg}}$ are the daily averages of CR and $i_b(k)$, respectively, while CL is the clearance[12]. To perform the regressors' choice, we resort to the stepwise regression technique, using the *Matlab* function stepwiselm. For $\widetilde{w}_2$, the selection principle we adopt is the Akaike Information Criterion (AIC), setting the maximum change of the computed AIC value to include a new regressor to the model to 0 and its minimal change to remove a term to 0.01; for the remaining hyperparameters, we use the Sum of Squared Errors (SSE) criterion, setting the maximum p-value of the F-statistic to add a new regressor to 0.05 and the minimal p-value to remove an element to 0.15. More details on the stepwise regression are reported in the appendix A.5. The final subsets of selected regressors are:

$$\varphi_{\tilde{r}_s}(p) = \varphi_{\tilde{r}_d}(p) = \varphi_{\tilde{r}_t}(p) = [1 \quad CR_{avg}(p) \quad BW(p)],$$

$$\varphi_{\tilde{s}_d}(p) = \varphi_{\tilde{s}_t}(p) = \varphi_{\widetilde{w}_1}(p) = [1 \quad CR_{avg}(p)],$$

$$\varphi_{\widetilde{w}_2}(p) = [1 \quad BW(p)].$$

The term 1 is added to include the intercept of the regression line.

Lastly, $\theta_h \in R^{N_{reg} \times 1}$ is the unknown vector of the regression model's parameters for the hyperparameters h and it is independent from which patient is considered, while $\epsilon_h(p)$ is the

[12] The blood volume per time unit that the kidneys clear from a substance, in the case from (inactive) insulin.

regression error. An estimate $\hat{\theta}_h$ of the model parameters can be computed by minimizing $\epsilon_h(p)$, thus:

$$\hat{\theta}_h = (\Phi^T\Phi)^{-1}\Phi^T\left[\log\left(h(1)\right) \quad \dots \quad \log\left(h(50)\right)\right]^T \quad (47)$$

where $\Phi \in R^{50\times N_{reg}}$ is the matrix obtained by concatenating the regressor vectors φ of the 50 patients of the training set. The achieved parameters $\hat{\theta}_h$ are:

$$\hat{\theta}_{\tilde{r}_s} = [4.0520, 0.2239, -0.0074]^T,$$
$$\hat{\theta}_{\tilde{r}_d} = [-2.3431, 0.3303, 0.0360]^T, \quad \hat{\theta}_{\tilde{s}_d} = [6.8416, 0.2689]^T,$$
$$\hat{\theta}_{\tilde{r}_t} = [2.8776, 0.3631, -0.0230]^T, \quad \hat{\theta}_{\tilde{s}_t} = [7.9909, 0.0763]^T,$$
$$\hat{\theta}_{\tilde{w}_1} = [-7.2072, 0.3878]^T, \quad \hat{\theta}_{\tilde{w}_2} = [3.2684, 0.0051]^T$$

for the standard simulation scenario, and

$$\hat{\theta}^R_{\tilde{r}_s} = [-2.9037, 0.2381, 0.0570]^T,$$
$$\hat{\theta}^R_{\tilde{r}_d} = [-5.8018, 0.3274, 0.0617]^T, \quad \hat{\theta}^R_{\tilde{s}_d} = [4.9214, 0.2724]^T,$$
$$\hat{\theta}^R_{\tilde{r}_t} = [-9.7427, 0.4326, 0.1020]^T, \quad \hat{\theta}^R_{\tilde{s}_t} = [8.7014, 0.0310]^T,$$
$$\hat{\theta}^R_{\tilde{w}_1} = [-5.0386, 0.1880]^T, \quad \hat{\theta}^R_{\tilde{w}_2} = [3.3945, 2.9283 \cdot 10^{-4}]^T$$

for the robustness test.

Finally, the regression laws can be used to obtain a suboptimal estimate of each hyperparameter, for any (virtual or real) patient l, as:

$$\hat{h}(l) = e^{\varphi_h(l)\hat{\theta}_h}. \quad (48)$$

V. Results and discussion

We report and discuss the results of our work, comparing those achieved with the triple-action MPC AP with those relative both to the single-action- and the dual-action MPC AP. We discriminate between the simulation scenario for the robustness test and the original one, i.e. with and without the additional persistent hyperglycaemias; for both the cases, we divide the results obtained with the optimal tuning, for the training set, from those achieved with the suboptimal parametrization, for the patients of the testing set. We confront the population distributions of the correspondent individualized hyperparameters and examined metrics, each described by its mean and standard deviation, if Gaussian, or by its median and interquartile range, otherwise. For the hyperparameters and a subset of fundamental metrics, we also include a figure, which integrates the two boxplots, the scatter plot and the parallel coordinate plot of the correspondent data obtained with the two algorithms being compared. By way of example, for each scenario, we show the results, in terms of simulated signals, obtained (with the optimal tuning) for a representative subject belonging to the training set, as well.

5.1. Original scenario

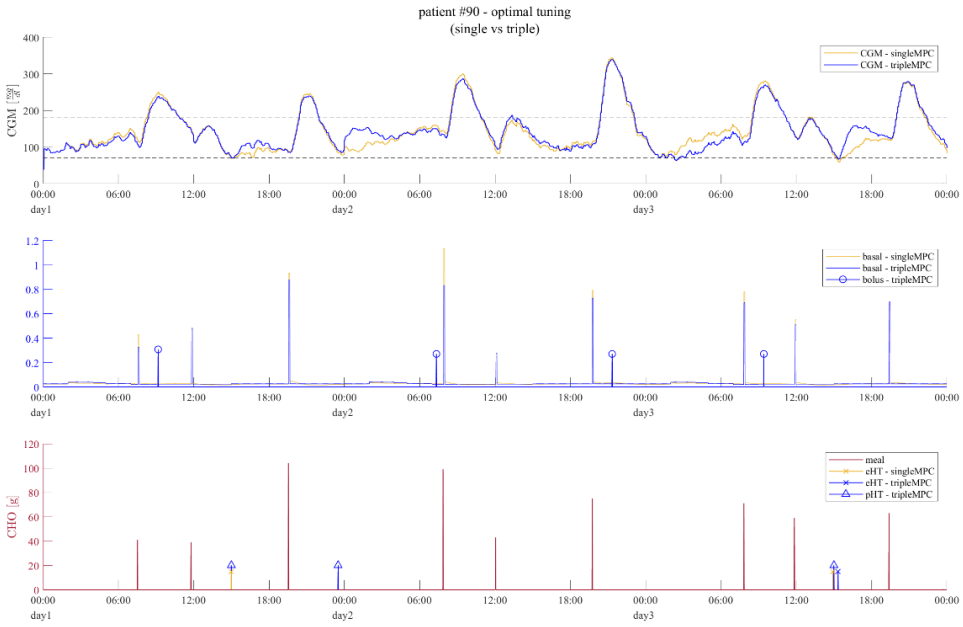

Figure 3. CGM measurements, basal insulin, corrective boluses, meals and hypotreatments (divided in emergency eHT and planned pHT), simulated on a representative patient, with the optimal tuning, in the original scenario. The yellow signals are referred to the singleMPC, while those in blue represent the tripleMPC. The black dashed lines in the CGM subplot (the first from above), are the borders of the euglycaemic range. The meals are in red.

Figure 3 shows the results of the three days of simulation on a representative patient (adult #90), in the original scenario, obtained with the singleMPC and the tripleMPC, both optimally tuned. The yellow lines refer to the former, while those in blue to the latter. From top to bottom,

the three subplots in this figure show respectively: the CGM signals; the administered basal insulin and the corrective boluses (identified by circles); the meals (red signal) and the hypotreatments, divided in emergency eHT (marked with a cross) and planned pHT (identified by triangles). This figure shows what we discussed in section III, i.e. that this simulation scenario is appropriate to test the single-action- and the dual-action MPC AP, but it is expected not to be the most suitable to test the actual potential of the triple-action MPC AP: in the hour and a half following each meal, no corrective boluses can be administered, and there are few other occasions where a bolus is needed. Consequently, the resultant performances of the two algorithms seem to be similar. Nonetheless, the potential of our technique can be already guessed from the fact that, even if not significantly, it still can counteract more the post-prandial hyperglycaemias, in particular those after breakfast, while avoiding important hypoglycaemic events, thanks to the planned extra-CHO intakes. Moreover, notice that most of the meal boluses computed by the tripleMPC are smaller, since they are integrated with the corrective boluses; therefore, insulin is better distributed in time.

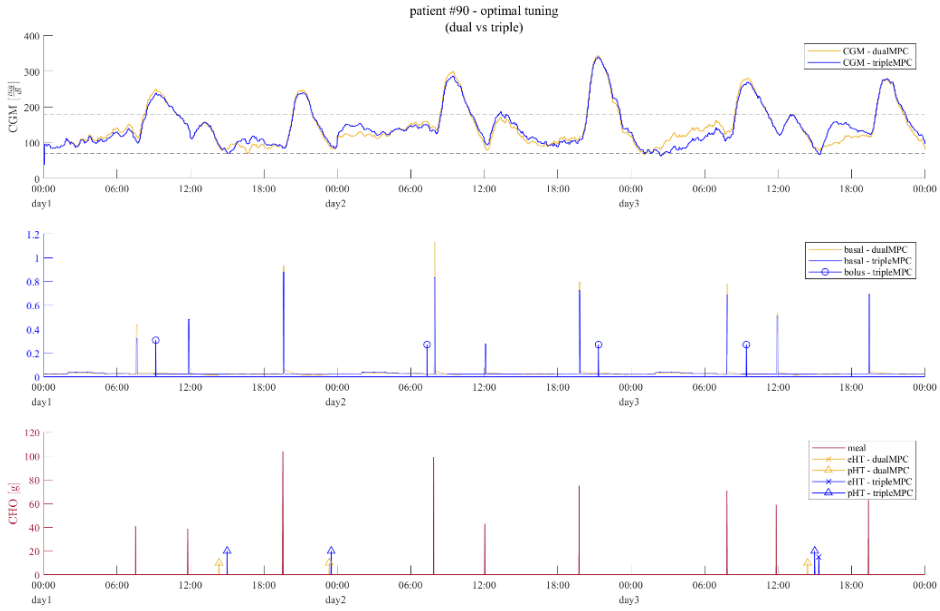

Figure 4. CGM measurements, basal insulin, corrective boluses, meals and hypotreatments (emergency and planned), on a representative patient, with the optimal tuning, in the original scenario. The yellow signals represent the dualMPC, while those in blue are related to the tripleMPC. The black dashed lines in the CGM subplot are the borders of the euglycaemic range. The meals are in red.

Figure 4 shows the results for the same representative patient, achieved (in the original scenario) with the dualMPC and the tripleMPC (with the optimal tuning). The yellow lines now refer to the dualMPC. The meaning of the plotted lines is the same as before. The remarks we can make are analogous to those for the previous plot: the triple-action MPC AP, thanks to the administration of more insulin, but more distributed in time, is capable of managing

hyperglycaemia in a (not significantly) better way. The control performances of the two strategies are almost comparable, as well as for their ability to avoid hypoglycaemia.

More complete results, both for the training set and the testing set, and a more detailed discussion are reported in the following.

Optimal tuning

Table V. Metrics and hyperparameters for the optimally tuned single- and tripleMPC (in the original scenario). For the normally distributed variables, identified by the symbol †, the mean ± the standard deviation is given, while for the others the median and the interquartile range ([$25^{th} - 75^{th}$ percentile]) are reported. The variables for which there is a statistically significant difference are identified by the symbol *, beside the p-value resultant from the relative statistical test.

training set			
Variable	singleMPC	tripleMPC	p-value
μ_{CGM} $\left[\frac{\text{mg}}{\text{dl}}\right]$	148.8 [139.9 − 158.6]	149.2 [140.4 − 156.1]	0.1602
$\sigma_{CGM}{}^{\dagger}$ $\left[\frac{\text{mg}}{\text{dl}}\right]$	54.1 ± 18.0	53.2 ± 17.7	0.2215
$TIR^{\dagger}$ [%]	76.6 ± 10.1	77.5 ± 9.0	0.2362
TBR [%]	0.1 [0.0 − 1.2]	0.1 [0.0 − 1.4]	0.4780
$TAR^{\dagger}$ [%]	22.7 ± 9.8	21.6 ± 8.6	0.0928
TDh [%]	0.0 [0.0 − 0.0]	0.0 [0.0 − 0.4]	0.1913
TDH [%]	7.1 [1.4 − 11.0]	6.6 [1.8 − 8.4]	0.0026 *
AUC_h $\left[\frac{\text{min}*\text{mg}}{\text{dl}}\right]$	1.0 [0.0 − 235.6]	0.6 [0.0 − 650.3]	0.3256
AUC_H $\left[\frac{\text{min}*\text{mg}}{\text{dl}}\right]$	$5.3 \cdot 10^4$ [$2.6 \cdot 10^4 - 7.0 \cdot 10^4$]	$4.8 \cdot 10^4$ [$2.3 \cdot 10^4 - 6.2 \cdot 10^4$]	0.0219 *
n_{HT}	0.1 [0.0 − 0.2]	0.3 [0.1 − 0.7]	$2.9 \cdot 10^{-5}$ *
n_{eHT}	-	0.1 [0.0 − 0.3]	-
n_{pHT}	-	0.2 [0.0 − 0.3]	-
q_{HT} [g]	1.9 [0.0 − 5.6]	5.3 [1.7 − 13.3]	$2.8 \cdot 10^{-5}$ *
q_{eHT} [g]	-	1.7 [0.0 − 7.2]	-
q_{pHT} [g]	-	3.6 [0.0 − 5.6]	-
n_{bol}	-	1.0 [0.3 − 1.7]	-
q_{bol} [U]	-	1.3 [0.5 − 2.2]	-
$TDI^{\dagger}$ [U]	40.9 ± 11.9	41.4 ± 12.5	2.2847
$\tilde{r}$ $\left[\left(\frac{\frac{\text{kg}}{\text{min}}}{\text{pmol}}\right)^2\right]$	$2.3 \cdot 10^3$ [$455.1 - 9.9 \cdot 10^3$]	$5.5 \cdot 10^3$ [$45.7 - 3.0 \cdot 10^5$]	0.2078
$\tilde{s}$	-	$7.4 \cdot 10^4$ [$8.5 \cdot 10^3 - 9.6 \cdot 10^4$]	-
$\widetilde{w}_1$ $\left[\left(\frac{\frac{\text{kg}}{\text{min}}}{\text{pmol}}\right)^2\right]$	-	6.6 [0.0 − 95.3]	-
$\widetilde{w}_2$	-	11.6 [2.9 − 563.5]	-

Table V shows how the metrics and the hyperparameters achieved (in the original simulation scenario) for the singleMPC and the tripleMPC, being optimally tuned, are distributed. For the variables that follow a Gaussian distribution (identified by the symbol †), the mean $\pm$ the standard deviation is reported, conversely for the others is more appropriate to indicate the median and the interquartile range ($[25^{\text{th}} - 75^{\text{th}}$ percentile]). The p-values resultant from the statistical tests, performed to compare the distributions of each variable for the two algorithms, are shown as well; beside a p-value the symbol * is indicated, if the distributions of the correspondent metric (or hyperparameter) are different in a statistically significant way. Notice that the time-in-range TIR is larger with our technique, even if not significantly, since the lowering of the time-below-range TBR and the time-above-range TAR are not remarkable, as guessed from figure 3. However, there is a statistically significant improvement for the time-in-deep-hyperglycaemia (and so for the area-under-the-curve in hyperglycaemia as well), showing the usefulness of the correction boluses even in the original scenario, which is not particularly suitable for testing the actual capabilities of the tripleMPC, as already discussed. There is a significant increase of the total number of hypotreatments n_{HT} as well, and also the total quantity of extra-CHO q_{HT}, that is expected due to the presence in our strategy of the planned hypotreatments.

In figure 5, the results for the metrics TIR, TBR, TAR, n_{HT} and the base 10 logarithm of the hyperparameter $\tilde{r}$ are shown in a more intuitive form, with two boxplots of the data obtained with the two algorithms, integrated with the scatter plot and the parallel coordinate plot of the same data. The differences in the variables can thus be appreciated for the single subjects as well. The segments of the parallel coordinate plot are coloured in green, if there is an improvement with our approach, otherwise in red (or in yellow, if the degradation is not significant); the darker the colour, the more significant the difference. The logarithm is applied to $\tilde{r}$ to have a linear and so more intelligible distribution. In this figure, it can be noticed that there is a significant part of the training set for which TAR, and thus TIR, increases with our technique, while TBR decreases.

In table VI the distributions of the same metrics and hyperparameters (in the same scenario) are reported for the optimally tuned dualMPC as well. The meanings of the symbols † and * are the same as for the previous table. In this case, TIR and TAR are comparable; this is due to the fact that the dualMPC can modulate the basal insulin in a slightly more aggressive way (indeed, $\tilde{r}$ tends to be significantly smaller, thus lowering the penalization on the basal insulin administration), thanks to presence of the planned hypotreatments, thus almost equalling the effect of the corrective boluses. The reason is to be attributed not to the fact the that the boluses

are ineffective, but that their usage is particularly limited, in the basic scenario. In addition, notice that, with the dualMPC, there is a quite inferior risk of hypoglycemia, and so a minor use of extra-CHO (indeed, n_{eHT}, q_{HT} and q_{eHT} are lower, and $\tilde{s}$ tends to be larger, therefore penalizing more the CHO suggestions).

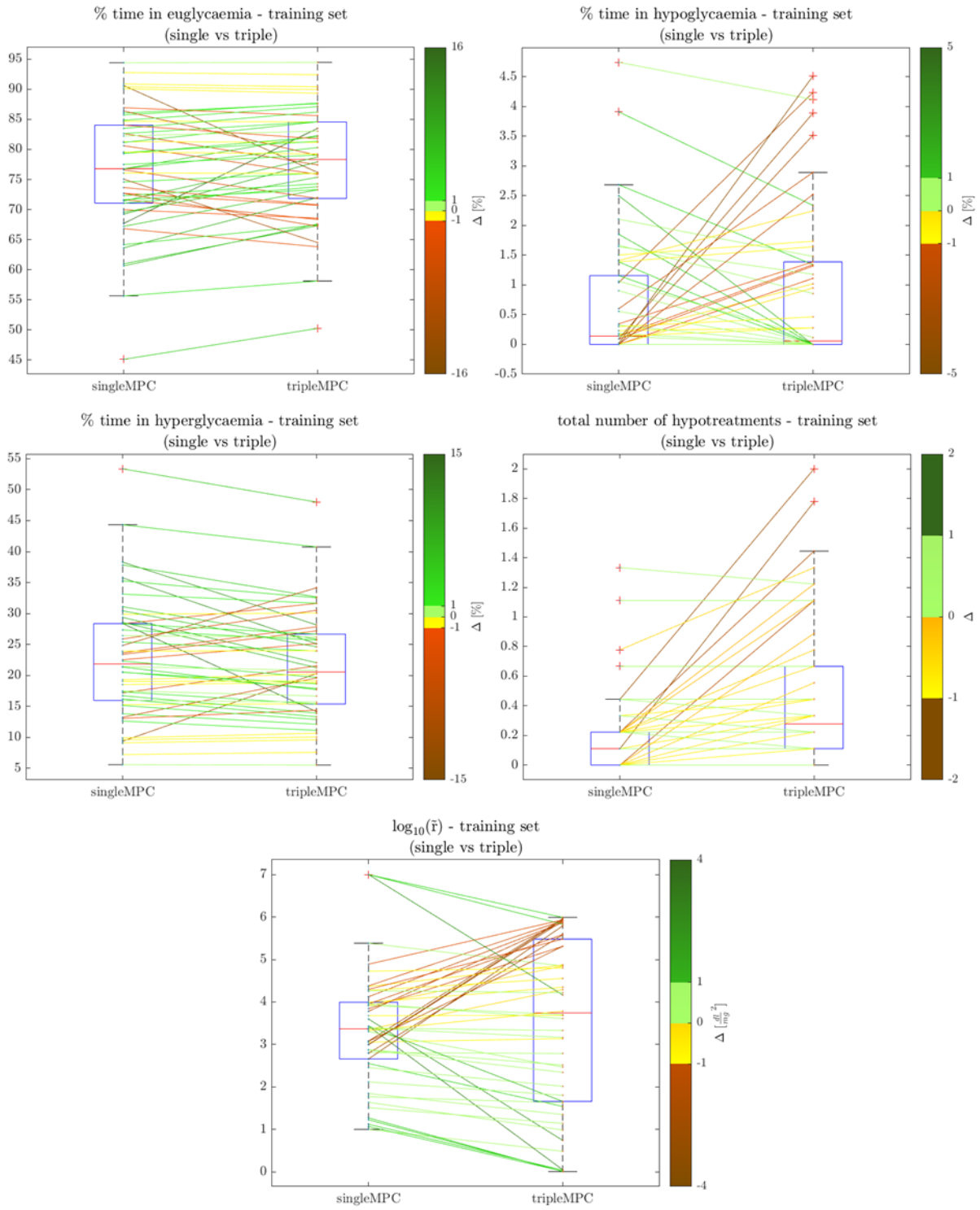

Figure 5. Boxplots, scatter plots and parallel coordinate plots for (from top to bottom, from left to right): TIR, TBR, TAR, n_{HT} and $log_{10}(\tilde{r})$, for the optimally tuned singleMPC and tripleMPC, in the original scenario. The segments of the parallel coordinate plot are green, if representing an improvement with the latter for the correspondent patient, otherwise are red (or yellow, if the degradation is not significant). The logarithm is applied to $\tilde{r}$ to have a linear distribution.

Table VI. Metrics and hyperparameters for the optimally tuned dual- and tripleMPC (in the basic scenario). For the variables which are normally distributed (symbol †), the mean ± the standard deviation is reported, while for the others the median and the interquartile range ([$25^{th} - 75^{th}$ percentile]) are indicated. The variables that differ in a statistically significant way are identified by the symbol *, beside the p-value resultant from the relative statistical test.

training set			
Variable	dualMPC	tripleMPC	p-value
μ_{CGM} $\left[\frac{\text{mg}}{\text{dl}}\right]$	149.6 [139.8 − 156.6]	149.2 [140.4 − 156.1]	0.8356
$\sigma_{CGM}{}^{\dagger}$ $\left[\frac{\text{mg}}{\text{dl}}\right]$	52.6 ± 17.2	53.2 ± 17.7	0.4064
$TIR^{\dagger}$ [%]	78.2 ± 9.2	77.5 ± 9.0	0.2835
TBR [%]	0.0 [0.0 − 0.5]	0.1 [0.0 − 1.4]	0.0248 *
$TAR^{\dagger}$ [%]	21.4 ± 8.8	21.6 ± 8.6	0.7104
TDh [%]	0.0 [0.0 − 0.0]	0.0 [0.0 − 0.4]	0.0011 *
TDH [%]	6.7 [1.3 − 9.1]	6.6 [1.8 − 8.4]	0.7535
AUC_h $\left[\frac{\text{min}*\text{mg}}{\text{dl}}\right]$	0.0 [0.0 − 27.4]	0.6 [0.0 − 650.3]	$7.6 \cdot 10^{-4}$ *
AUC_H $\left[\frac{\text{min}*\text{mg}}{\text{dl}}\right]$	$4.72 \cdot 10^4$ [$2.5 \cdot 10^4 - 6.4 \cdot 10^4$]	$4.8 \cdot 10^4$ [$2.3 \cdot 10^4 - 6.2 \cdot 10^4$]	0.9577
n_{HT}	0.7 [0.0 − 2.0]	0.3 [0.1 − 0.7]	0.6540
n_{eHT}	0.0 [0.0 − 0.3]	0.1 [0.0 − 0.3]	0.0027 *
n_{pHT}	0.2 [0.0 − 1.3]	0.2 [0.0 − 0.3]	0.3244
q_{HT} [g]	10.0 [0.0 − 21.7]	5.3 [1.7 − 13.3]	0.0070 *
q_{eHT} [g]	0.0 [0.0 − 8.3]	1.7 [0.0 − 7.2]	0.0028 *
q_{pHT} [g]	1.7 [0.0 − 13.3]	3.6 [0.0 − 5.6]	0.0722
n_{bol}	-	1.0 [0.3 − 1.7]	-
q_{bol} [U]	-	1.3 [0.5 − 2.2]	-
$TDI^{\dagger}$ [U]	42.1 ± 13.2	41.4 ± 12.5	0.0828
$\tilde{r}$ $\left[\left(\frac{\frac{\text{kg}}{\text{min}}}{\text{pmol}}\right)^2\right]$	$1.2 \cdot 10^3$ [$43.8 - 8.8 \cdot 10^3$]	$5.5 \cdot 10^3$ [$45.7 - 3.0 \cdot 10^5$]	0.0208 *
$\tilde{s}$	$2.1 \cdot 10^5$ [$4.1 \cdot 10^3 - 3.8 \cdot 10^7$]	$7.4 \cdot 10^4$ [$8.5 \cdot 10^3 - 9.6 \cdot 10^4$]	$2.1 \cdot 10^{-4}$ *
$\widetilde{w}_1$ $\left[\left(\frac{\frac{\text{kg}}{\text{min}}}{\text{pmol}}\right)^2\right]$	-	6.6 [0.0 − 95.3]	-
$\widetilde{w}_2$	-	11.6 [2.9 − 563.5]	-

Figure 6 is analogous to the previous one, but it is referred to the comparison between the tripleMPC and the dual-action strategy, with optimal tuning, in the original simulation scenario. In addition, there is the boxplot, together with the scatter and the parallel coordinate plots, of the data regarding n_{eHT}, n_{pHT} and base 10 logarithm of $\tilde{s}$, as well. The logarithm is applied to $\tilde{s}$ for the same reason as for $\tilde{r}$. Basing on this figure, we can remark that the performances of the two algorithms, in the currently considered scenario, are substantially similar.

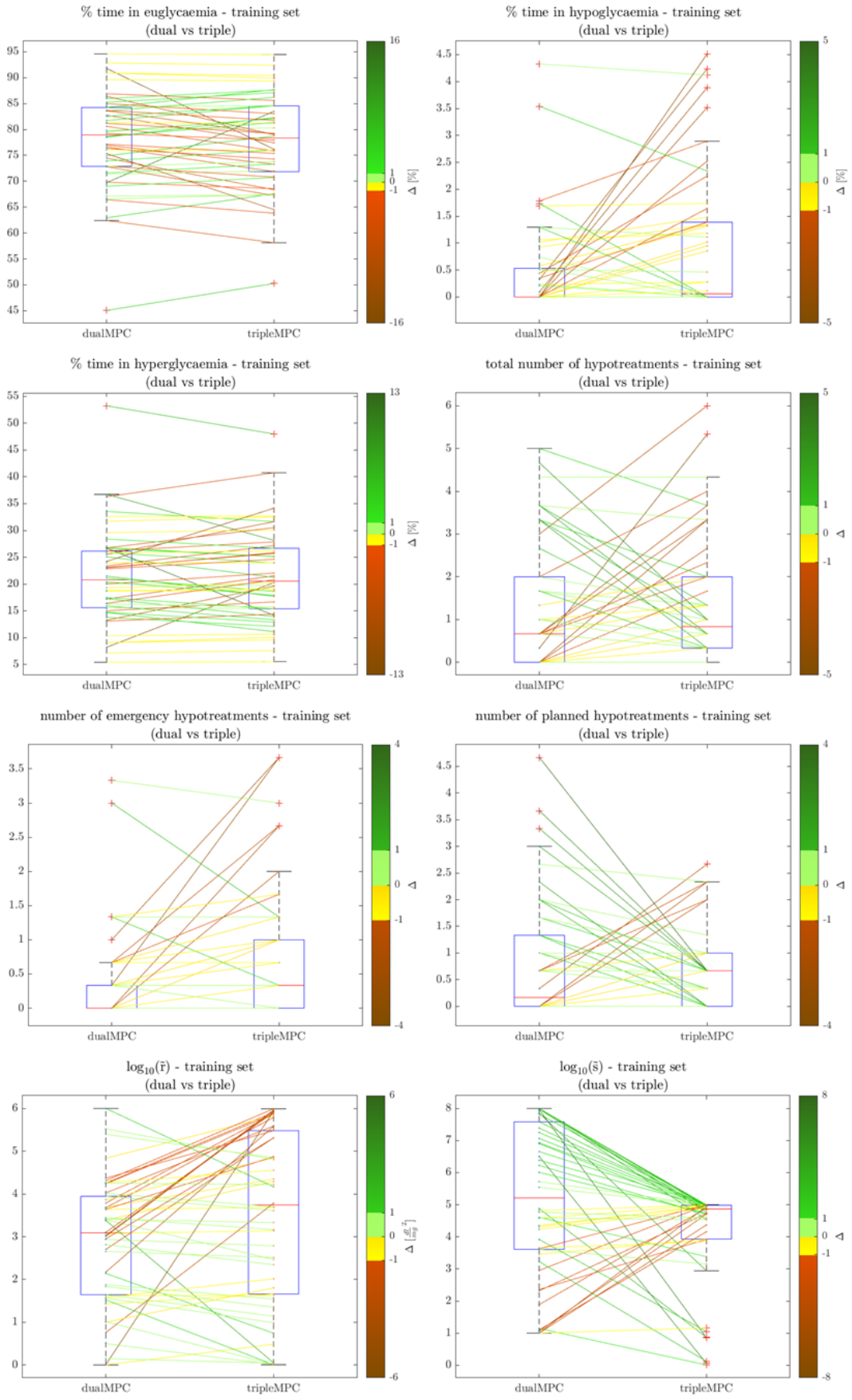

Figure 6. Boxplots, scatter plots and parallel coordinate plots for (from top to bottom, from left to right): TIR, TBR, TAR, n_{HT}, n_{eHT}, n_{pHT}, $log_{10}(\tilde{r})$ and $log_{10}(\tilde{s})$, for the optimally tuned dual- and tripleMPC (in the original scenario). The segments of the parallel coordinate plot are green, if representing an improvement with the latter for the correspondent patient, otherwise are red (or yellow, if the degradation is not significant). The logarithm is applied to $\tilde{r}$ and $\tilde{s}$ to have a linear distribution.

Suboptimal tuning

Table VII. Metrics and hyperparameters for the single- and the tripleMPC (in the original scenario), with suboptimal tuning. For the variables with a Gaussian distribution (symbol †), the mean ± the standard deviation is reported, while for the others the median and the interquartile range ($[25^{th} - 75^{th}$ percentile]). The variables for which there is a statistically significant difference are identified by the symbol *, beside the p-value resultant from the relative statistical test.

testing set			
Variable	singleMPC	tripleMPC	p-value
μ_{CGM} $\left[\frac{\text{mg}}{\text{dl}}\right]$	$153.9\ [141.0 - 170.4]$	$154.4\ [143.0 - 169.3]$	0.0101 *
$\sigma_{CGM}{}^{\dagger}$ $\left[\frac{\text{mg}}{\text{dl}}\right]$	54.3 ± 18.5	58.8 ± 22.1	$6.3 \cdot 10^{-5}$ *
$TIR^{\dagger}$ [%]	73.8 ± 11.8	71.6 ± 13.6	0.0071 *
TBR [%]	$0.0\ [0.0\ -\ 1.1]$	$1.0\ [0.0\ -\ 3.4]$	$2.7 \cdot 10^{-4}$ *
$TAR^{\dagger}$ [%]	25.5 ± 11.3	26.4 ± 11.8	0.1023
TDh [%]	$0.0\ [0.0 - 0.0]$	$0.0\ [0.0 - 1.0]$	$1.6 \cdot 10^{-4}$ *
TDH [%]	$7.4\ [1.7 - 13.1]$	$7.8\ [2.3 - 15.7]$	0.0042 *
AUC_h $\left[\frac{\text{min}*\text{mg}}{\text{dl}}\right]$	$0.0\ [0.0 - 301.2]$	$489.9\ [0.0 - 1.4 \cdot 10^3]$	$3.7 \cdot 10^{-5}$ *
AUC_H $\left[\frac{\text{min}*\text{mg}}{\text{dl}}\right]$	$6.6 \cdot 10^4\ [2.5 \cdot 10^4 - 1.0 \cdot 10^5]$	$6.4 \cdot 10^4\ [2.7 \cdot 10^4 - 1.1 \cdot 10^5]$	0.0024 *
n_{HT}	$0.0\ [0.0 - 0.2]$	$0.5\ [0.3 - 1.3]$	$1.5 \cdot 10^{-9}$ *
n_{eHT}	-	$0.1\ [0.0 - 0.7]$	-
n_{pHT}	-	$0.4\ [0.3 - 0.4]$	-
q_{HT} [g]	$0.0\ [0.0 - 3.9]$	$8.9\ [5.6 - 24.4]$	$1.1 \cdot 10^{-9}$ *
q_{eHT} [g]	-	$2.2\ [0.0 - 13.3]$	-
q_{pHT} [g]	-	$7.2\ [5.0 - 8.3]$	-
$n_{bol}{}^{\dagger}$	-	2.5 ± 1.6	-
$q_{bol}{}^{\dagger}$ [U]	-	3.8 ± 2.7	-
$TDI^{\dagger}$ [U]	39.5 ± 10.1	39.0 ± 10.3	0.0510
$\tilde{r}$ $\left[\left(\frac{\frac{\text{kg}}{\text{min}}}{\text{pmol}}\right)^2\right]$	$2.9 \cdot 10^3\ [899.1 - 7.8 \cdot 10^3]$	$4.7 \cdot 10^3\ [631.8 - 1.9 \cdot 10^4]$	$1.4 \cdot 10^{-4}$ *
$\tilde{s}$	-	$1.3 \cdot 10^4\ [9.3 \cdot 10^3 - 2.0 \cdot 10^4]$	-
$\widetilde{w}_1$ $\left[\left(\frac{\frac{\text{kg}}{\text{min}}}{\text{pmol}}\right)^2\right]$	-	$1.5\ [0.2 - 12.04]$	-
$\widetilde{w}_2$	-	$38.5\ [36.8 - 40.0]$	-

We now compare the performances of the singleMPC and the tripleMPC, evaluated in the basic scenario on the testing set, with the suboptimal hyperparameters (inferred by using the regression models presented in section IV). Confronting the metrics' distributions reported in tables V and VII, we assist to a degradation of the performances for both the algorithms, which is expected, since the regression laws are approximate. However, this is more evident for the tripleMPC: e.g., the decrease of the average TIR is 5.9 units, while for the singleMPC it is 2.8

units. This is why the quality of control of our technique is quite worse, with a slightly longer time spent in hypoglycaemia and, therefore, a significant increase of the hypotreatments, as shown in table VII. The principal reason of this is probably the lower quality of the regression model for the hyperparameter $\widetilde{w}_2$: indeed, the second term of the vector $\hat{\theta}_{\widetilde{w}_2}$ (reported in section IV) is relatively small, which means that the variable BW is not a significant regressor for $\widetilde{w}_2$ (despite being selected by stepwise regression); therefore, the variability of $\widetilde{w}_2$ is not sufficiently nor appropriately explained.

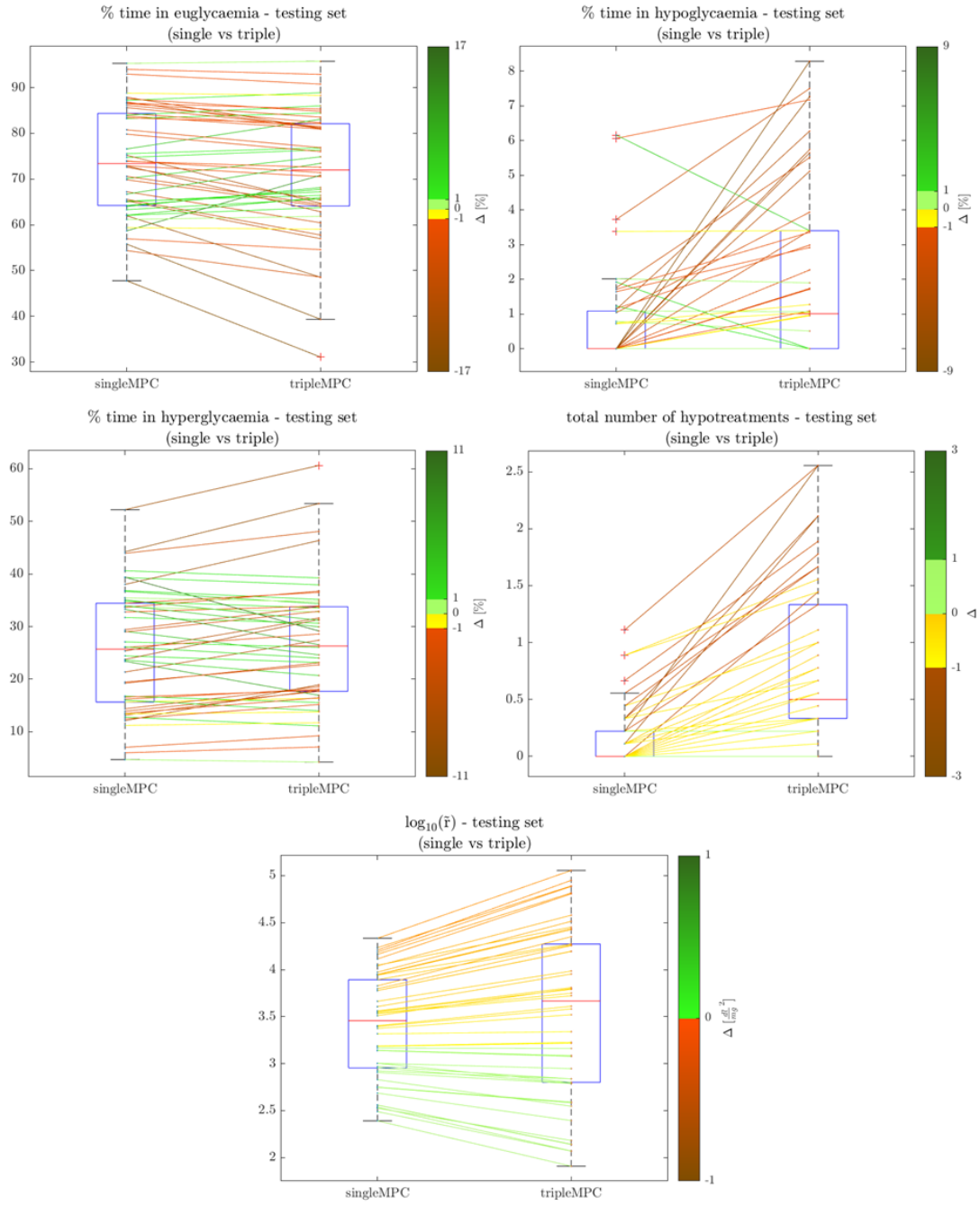

Figure 7. Boxplots, scatter plots and parallel coordinate plots for (from top to bottom, from left to right): TIR, TBR, TAR, n_{HT} and $log_{10}(\tilde{r})$, for the sub-optimally tuned single- and tripleMPC (in the original scenario). The segments of the parallel coordinate plot are green, if representing an improvement with the latter for the correspondent patient, otherwise are red (or yellow, if the degradation is not significant). The logarithm is applied to $\tilde{r}$ to have a linear distribution.

Figure 7 shows the integration of boxplots, scatter plot and parallel coordinate plot for the data referred to the sub-optimally tuned singleMPC and tripleMPC, in the currently considered scenario, and supports the previous remarks. In this scenario, if our algorithm is employed with a suboptimal parametrization, is less effective than its optimally tuned version, since the number of patients in the testing set for which there is a degradation of the control quality, being compared to the singleMPC, is larger, with respect to the training set.

Table VIII. Metrics and hyperparameters for the sub-optimally tuned dual- and tripleMPC, in the basic scenario. For the variables which are normally distributed (symbol †), the mean ± the standard deviation is reported, while for the others the median and the interquartile range ([$25^{th} - 75^{th}$ percentile]) are indicated. The variables that differ in a statistically significant way are identified by the symbol *, beside the p-value resultant from the relative statistical test.

testing set			
Variable	dualMPC	tripleMPC	p-value
μ_{CGM} $\left[\frac{\text{mg}}{\text{dl}}\right]$	$153.7\ [139.1 - 167.4]$	$154.4\ [143.0 - 169.3]$	$6.8 \cdot 10^{-5}$ *
$\sigma_{CGM}{}^{\dagger}$ $\left[\frac{\text{mg}}{\text{dl}}\right]$	53.7 ± 18.5	58.8 ± 22.1	$2.6 \cdot 10^{-6}$ *
$TIR^{\dagger}$ [%]	74.6 ± 12.0	71.6 ± 13.6	$1.7 \cdot 10^{-4}$ *
TBR [%]	$0.0\ [0.0\ -\ 1.2]$	$1.0\ [0.0\ -\ 3.4]$	$7.2 \cdot 10^{-4}$ *
$TAR^{\dagger}$ [%]	24.5 ± 11.4	26.4 ± 11.8	0.0013 *
TDh [%]	$0.0\ [0.0 - 0.0]$	$0.0\ [0.0 - 1.0]$	$1.6 \cdot 10^{-4}$ *
TDH [%]	$7.1\ [1.7 - 12.7]$	$7.8\ [2.3 - 15.7]$	$8.5 \cdot 10^{-5}$ *
AUC_h $\left[\frac{\text{min}*\text{mg}}{\text{dl}}\right]$	$0.0\ [0.0 - 352.1]$	$489.9\ [0.0 - 1.4 \cdot 10^3]$	$1.1 \cdot 10^{-4}$ *
AUC_H $\left[\frac{\text{min}*\text{mg}}{\text{dl}}\right]$	$6.2 \cdot 10^4\ [2.1 \cdot 10^4 - 9.7 \cdot 10^4]$	$6.4 \cdot 10^4\ [2.7 \cdot 10^4 - 1.1 \cdot 10^5]$	$1.1 \cdot 10^{-5}$ *
n_{HT}	$0.1\ [0.0 - 0.3]$	$0.5\ [0.3 - 1.3]$	$2.4 \cdot 10^{-9}$ *
n_{eHT}	$0.0\ [0.0 - 0.2]$	$0.1\ [0.0 - 0.7]$	$2.3 \cdot 10^{-4}$ *
n_{pHT}	$0.0\ [0.0 - 0.0]$	$0.4\ [0.3 - 0.4]$	$2.4 \cdot 10^{-9}$ *
q_{HT} [g]	$1.7\ [0.0 - 5.6]$	$8.9\ [5.6 - 24.4]$	$1.0 \cdot 10^{-9}$ *
q_{eHT} [g]	$0.0\ [0.0 - 5.6]$	$2.2\ [0.0 - 13.3]$	$9.6 \cdot 10^{-5}$ *
q_{pHT} [g]	$0.0\ [0.0 - 0.0]$	$7.2\ [5.0 - 8.3]$	$1.2 \cdot 10^{-9}$ *
$n_{bol}{}^{\dagger}$	-	2.5 ± 1.6	-
$q_{bol}{}^{\dagger}$ [U]	-	3.8 ± 2.7	-
$TDI^{\dagger}$ [U]	40.0 ± 10.6	39.0 ± 10.3	$8.0 \cdot 10^{-5}$ *
$\tilde{r}$ $\left[\left(\frac{\frac{\text{kg}}{\text{min}}}{\text{pmol}}\right)^2\right]$	$791.4\ [224.9 - 3.7 \cdot 10^3]$	$4.7 \cdot 10^3\ [631.8 - 1.9 \cdot 10^4]$	$2.3 \cdot 10^{-8}$ *
$\tilde{s}$	$1.8 \cdot 10^5\ [5.3 \cdot 10^4 - 7.8 \cdot 10^5]$	$1.3 \cdot 10^4\ [9.3 \cdot 10^3 - 2.0 \cdot 10^4]$	$7.4 \cdot 10^{-10}$ *
$\widetilde{w}_1$ $\left[\left(\frac{\frac{\text{kg}}{\text{min}}}{\text{pmol}}\right)^2\right]$	-	$1.5\ [0.2 - 12.04]$	-
$\widetilde{w}_2$	-	$38.5\ [36.8 - 40.0]$	-

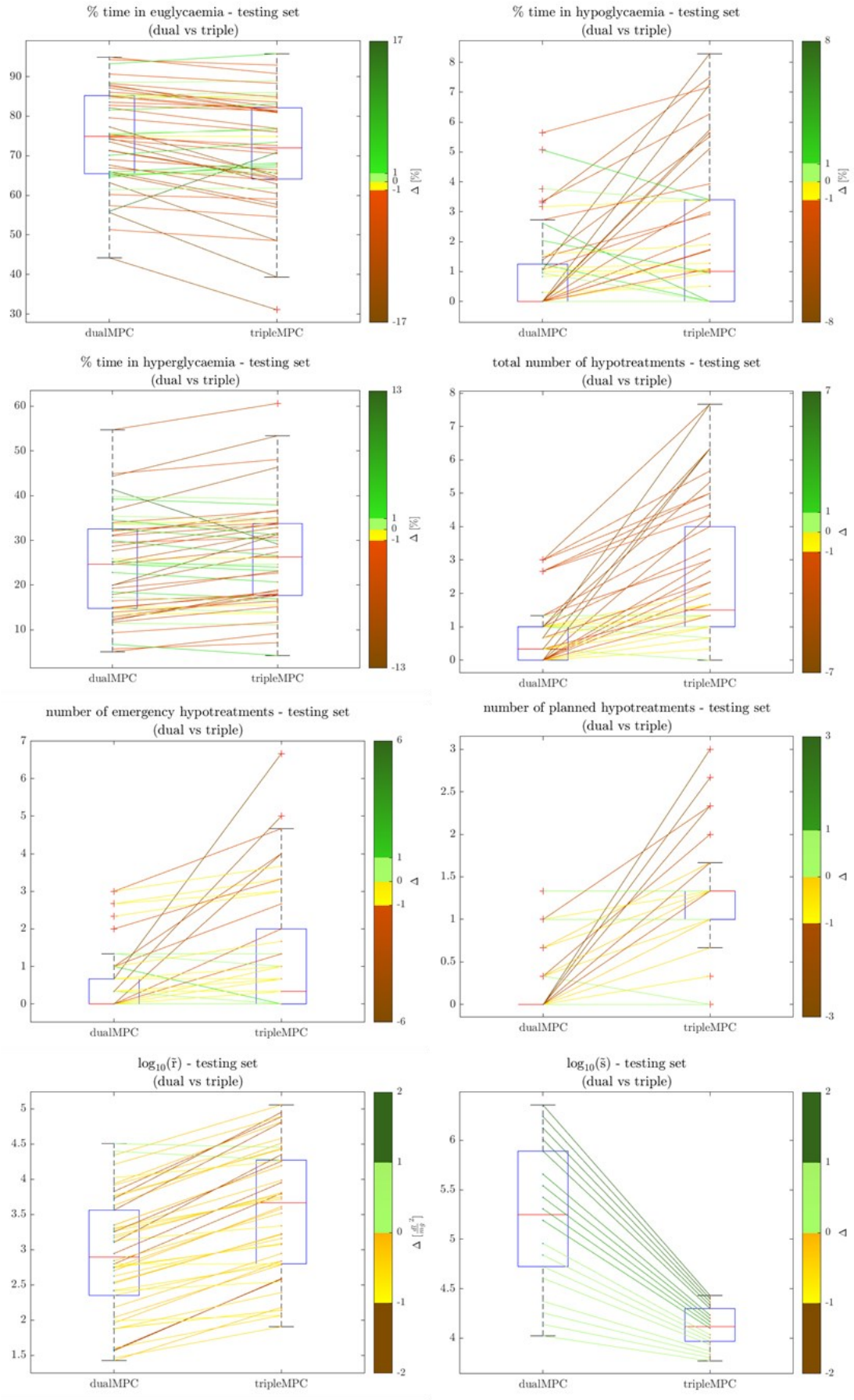

Figure 8. Boxplots, scatter plots and parallel coordinate plots for (from top to bottom, from left to right): TIR, TBR, TAR, n_{HT}, n_{eHT}, n_{pHT}, $log_{10}(\tilde{r})$ and $log_{10}(\tilde{s})$, for the dual- and the tripleMPC (in the original scenario), with suboptimal tuning. The segments of the parallel coordinate plot are green, if representing an improvement with the latter for the correspondent patient, otherwise are red (or yellow, if the degradation is not significant).

Table VIII and figure 8 show the results obtained with the suboptimal tuning of the dual-action- and the triple-action MPC AP. In this case, the consequences of the approximation error of the regression model for $\widetilde{w}_2$, added to the fact that the current scenario is not the most suitable to test our strategy (while being appropriate for the dualMPC, and the singleMPC as well), are more evident. The tripleMPC is quite less effective, the difference of each metric is statistically significant and, particularly for the metrics reported in figure 8, there is no improvement for most of the testing set.

We can conclude that the regression of the hyperparameters for the tripleMPC, particularly of $\widetilde{w}_2$, must be refined, and that, as expected, the original scenario is not the most suitable to evaluate the actual usefulness of our algorithm. However, the results achieved with its optimally tuned version suggest its potential, and particularly its capability to effectively counteract hyperglycaemia, without significantly increasing the risk of incurring in hypoglycaemic events. This will be much more appreciable in the following section, where we report the results obtained in the simulation scenario including the additional persistent hyperglycaemias.

5.2. Robustness test

Figures 9 and 10 show the simulated signals obtained employing the tripleMPC on the representative patient (#90), compared to those achieved (for the same subject) with the singleMPC and the dualMPC, respectively. The considered scenario is the advanced one (i.e., comprehending the additional persistent hyperglycaemias), and the hyperparameters of the algorithms are optimal. Since no extra boluses can be administered after a meal, as already discussed, the quality of control of the post-prandial hyperglycaemias of the three algorithms is comparable. However, a significant difference can be noticed in the rest of the simulated period, particularly between about $01{:}00$ AM and $07{:}00$ AM, when the persistent hyperglycaemic events occur: indeed, even if these events are unexplained and unannounced, our algorithm is able to solve them (particularly during the second night), thanks exactly to the corrective boluses, while this is not possible with the basal insulin modulation, which is the only strategy the single- and the dualMPC can resort to. Apart from the post-prandial times, with the tripleMPC the glucose level is maintained almost completely in euglycaemia. Even if the generation mechanism of the nocturnal hyperglycaemias (as explained in section III) is not properly realistic (and must be revised), the introduction of such a type of events makes sense, since they are persistent, as well as the real hyperglycaemias typically are, and occur apart from mealtimes, as in the real cases of hyperglycaemic events due to additional disturbing factors,

e.g., stress or alcohol assumption. Therefore, the results reported in these two figures are a first demonstration of the real usefulness of our innovative approach, in such a more challenging and possibly more realistic scenario.

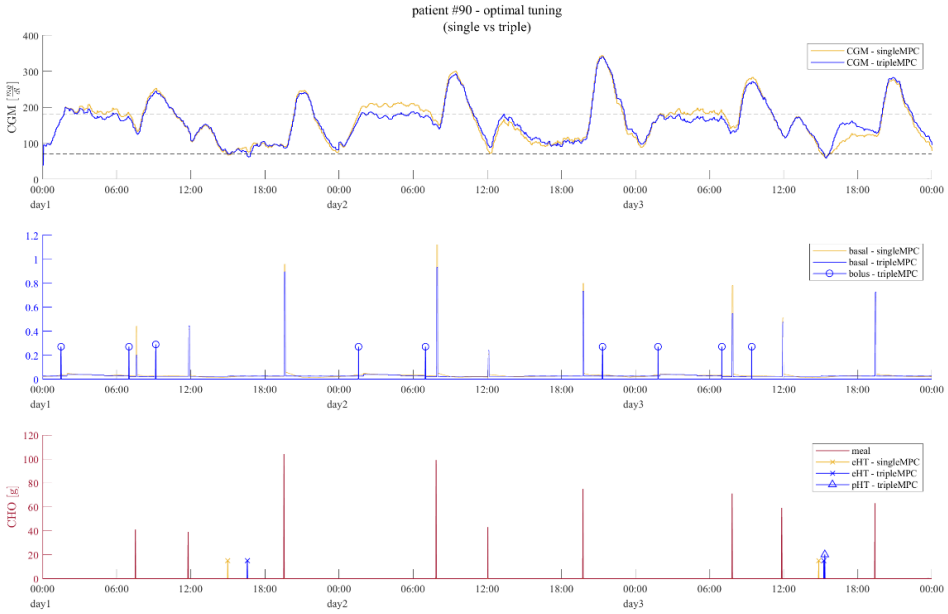

Figure 9. CGM measurements, basal insulin, corrective boluses, meals and hypotreatments (divided in emergency eHT and planned pHT), simulated on subject #90, with the optimal tuning, in the advanced scenario. The yellow signals are referred to the singleMPC, while those in blue represent the tripleMPC. The black dashed lines in the CGM subplot are the borders of the euglycaemic range. The meals are in red.

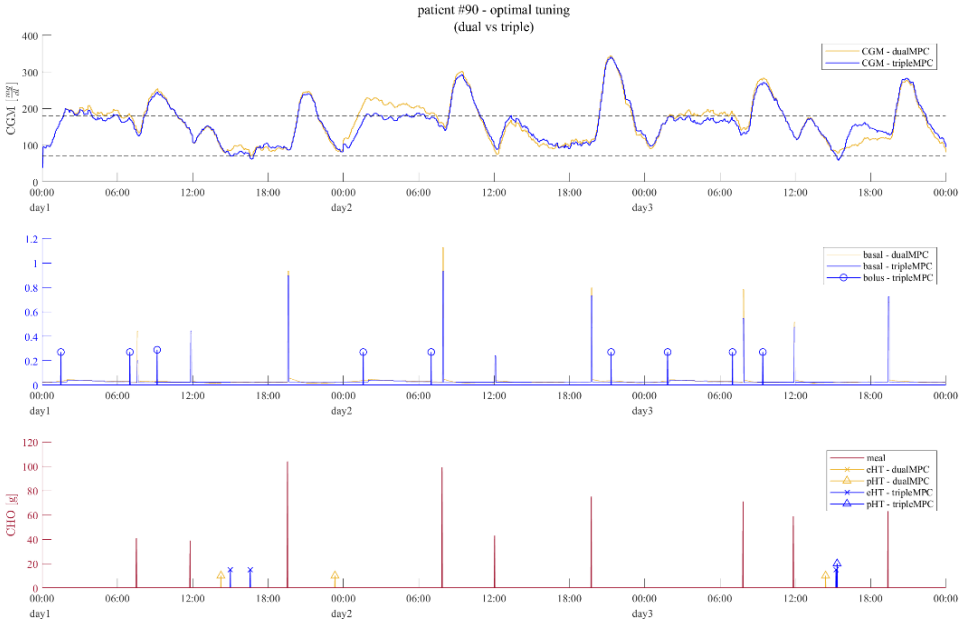

Figure 10. CGM measurements, basal insulin, corrective boluses, meals and hypotreatments (eHT and pHT), simulated on subject #90, with the optimal tuning, in the scenario for the robustness test. The yellow signals respresent the dualMPC, those in blue are referred to the tripleMPC. The black dashed lines in the CGM subplot are the borders of the euglycaemic range. The meals are in red.

The population results for the advanced scenario and a more complete discussion are present in the following.

Optimal tuning

The comparison of the population distribution of the metrics and the hyperparameters of the tripleMPC with those referred to the singleMPC and the dualMPC, evaluated in the advanced scenario on the training set (with optimal tuning), is described by the values in tables IX and X, respectively.

Table IX. Metrics and hyperparameters for the optimally tuned single- and tripleMPC (in the advanced scenario). For the normally distributed variables, identified by the symbol †, the mean ± the standard deviation is given, while for the others the median and the interquartile range ([$25^{th} - 75^{th}$ percentile]) are reported. The variables for which there is a statistically significant difference are identified by the symbol *, beside the p-value resultant from the relative statistical test.

training set			
Variable	singleMPC	tripleMPC	p-value
μ_{CGM} $\left[\frac{\text{mg}}{\text{dl}}\right]$	$170.3\ [158.8 - 182.0]$	$164.9\ [154.8 - 176.7]$	$1.3 \cdot 10^{-4}$ *
σ_{CGM} $\left[\frac{\text{mg}}{\text{dl}}\right]$	$57.1\ [50.1 - 68.0]$	$54.2\ [45.0 - 60.6]$	$1.8 \cdot 10^{-5}$ *
$TIR^{\dagger}$ [%]	57.0 ± 11.9	62.2 ± 12.5	$3.0 \cdot 10^{-5}$ *
TBR [%]	$0.9\ [0.0\ -\ 2.0]$	$0.8\ [0.0 -\ 2.0]$	0.0860
$TAR^{\dagger}$ [%]	41.8 ± 11.4	36.6 ± 12.2	$7.0 \cdot 10^{-5}$ *
TDh [%]	$0.0\ [0.0 - 0.7]$	$0.0\ [0.0 - 0.6]$	0.4756
TDH [%]	$10.4\ [3.8 - 17.1]$	$7.1\ [1.8 - 13.1]$	$3.5 \cdot 10^{-6}$ *
AUC_h $\left[\frac{\text{min}*\text{mg}}{\text{dl}}\right]$	$175.2\ [0.0 - 916.1]$	$153.4\ [0.0 - 840.2]$	0.0903
AUC_H $\left[\frac{\text{min}*\text{mg}}{\text{dl}}\right]$	$8.7 \cdot 10^4\ [5.5 \cdot 10^4 - 1.2 \cdot 10^5]$	$6.7 \cdot 10^4\ [4.2 \cdot 10^4 - 1.0 \cdot 10^5]$	$3.5 \cdot 10^{-7}$ *
n_{HT}	$0.2\ [0.0 - 0.6]$	$0.4\ [0.1 - 1.0]$	$7.8 \cdot 10^{-4}$ *
n_{eHT}	-	$0.1\ [0.0 - 0.4]$	-
n_{pHT}	-	$0.2\ [0.0 - 0.3]$	-
q_{HT} [g]	$3.3\ [0.0 - 10.0]$	$6.9\ [1.7 - 17.8]$	0.0021 *
q_{eHT} [g]	-	$2.8\ [0.0 - 8.9]$	-
q_{pHT} [g]	-	$2.8\ [0.0 - 6.7]$	-
${n_{bol}}^{\dagger}$	-	2.6 ± 1.9	-
${q_{bol}}^{\dagger}$ [U]	-	3.3 ± 2.5	-
$TDI^{\dagger}$ [U]	45.4 ± 13.3	44.3 ± 14.6	0.0566
$\tilde{r}$ $\left[\left(\frac{\frac{\text{kg}}{\text{min}}}{\text{pmol}}\right)^2\right]$	$432.4\ [50.8 - 1.2 \cdot 10^3]$	$415.2\ [3.2 - 8.6 \cdot 10^4]$	0.2184
$\tilde{s}$	-	$6.6 \cdot 10^4\ [8.2 \cdot 10^3 - 9.9 \cdot 10^4]$	-
$\widetilde{w}_1$ $\left[\left(\frac{\frac{\text{kg}}{\text{min}}}{\text{pmol}}\right)^2\right]$	-	$0.15\ [0.0 - 25.9]$	-
$\widetilde{w}_2$	-	$11.4\ [2.6 - 224.1]$	-

Basing on table IX, we observe a net improvement of control with our technique, with respect to the single-action approach: the time-above-range TAR decreases in a statistically significant

way, as well as the time-in-deep-hyperglycaemia TDH and the mean CGM signal μ_{CGM}, despite using a lower total quantity of insulin (indeed, the daily average quantity, TDI, is minor). This means that there is a better distribution in time of the administered insulin, possibly with a higher concentration only when needed (thanks to the boluses). In addition, the time-below-range TBR is lower as well (almost significantly, since the threshold p-value is 5%), for a major employment of hypotreatments, which is expected. Overall, with the tripleMPC, the total time-in-range TIR is subject to an increase, on average, of 9.1% (with respect to the value obtained with the singleMPC).

Table X. Metrics and hyperparameters for dual- and tripleMPC, in the advanced scenario, with optimal tuning. For the variables with a Gaussian distribution (the symbol †), the mean ± the standard deviation is reported, while for the others the median and the interquartile range ($[25^{th} - 75^{th}$ percentile]).

training set			
Variable	dualMPC	tripleMPC	p-value
μ_{CGM} $\left[\frac{\text{mg}}{\text{dl}}\right]$	166.7 [158.6 − 176.0]	164.9 [154.8 − 176.7]	0.7758
σ_{CGM} $\left[\frac{\text{mg}}{\text{dl}}\right]$	56.3 [47.2 − 63.0]	54.2 [45.0 − 60.6]	0.0591
$TIR^{\dagger}$ [%]	60.5 ± 11.6	62.2 ± 12.5	0.1166
TBR [%]	0.3 [0.0 − 1.6]	0.8 [0.0 − 2.0]	0.1483
$TAR^{\dagger}$ [%]	38.6 ± 11.3	36.6 ± 12.2	0.0884
TDh [%]	0.0 [0.0 − 0.0]	0.0 [0.0 − 0.6]	0.1528
TDH [%]	8.0 [1.5 − 13.7]	7.1 [1.8 − 13.1]	0.7527
AUC_h $\left[\frac{\text{min}*\text{mg}}{\text{dl}}\right]$	9.8 [0.0 − 593.9]	153.4 [0.0 − 840.2]	0.2580
AUC_H $\left[\frac{\text{min}*\text{mg}}{\text{dl}}\right]$	$7.4 \cdot 10^4$ [$5.2 \cdot 10^4 - 1.0 \cdot 10^5$]	$6.7 \cdot 10^4$ [$4.2 \cdot 10^4 - 1.0 \cdot 10^5$]	0.2009
n_{HT}	1.0 [0.3 − 4.0]	0.4 [0.1 − 1.0]	0.0352 *
n_{eHT}	0.3 [0.0 − 1.0]	0.1 [0.0 − 0.4]	0.1183
n_{pHT}	1.0 [0.0 − 2.7]	0.2 [0.0 − 0.3]	0.0028 *
q_{HT} [g]	13.3 [5.0 − 45.0]	6.9 [1.7 − 17.8]	0.8866
q_{eHT} [g]	5.0 [0.0 − 16.7]	2.8 [0.0 − 8.9]	0.2151
q_{pHT} [g]	10.0 [0.0 − 25.0]	2.8 [0.0 − 6.7]	0.7270
$n_{bol}{}^{\dagger}$	-	2.6 ± 1.9	-
$q_{bol}{}^{\dagger}$ [U]	-	3.3 ± 2.5	-
$TDI^{\dagger}$ [U]	48.0 ± 15.5	44.3 ± 14.6	$6.3 \cdot 10^{-8}$ *
$\tilde{r}$ $\left[\left(\frac{\frac{\text{kg}}{\text{min}}}{\text{pmol}}\right)^2\right]$	222.9 [$10.4 - 2.0 \cdot 10^3$]	415.2 [$3.2 - 8.6 \cdot 10^4$]	0.0083 *
$\tilde{s}$	$1.8 \cdot 10^4$ [$202.1 - 1.2 \cdot 10^6$]	$6.6 \cdot 10^4$ [$8.2 \cdot 10^3 - 9.9 \cdot 10^4$]	0.1876
$\widetilde{w}_1$ $\left[\left(\frac{\frac{\text{kg}}{\text{min}}}{\text{pmol}}\right)^2\right]$	-	0.15 [0.0 − 25.9]	-
$\widetilde{w}_2$	-	11.4 [2.6 − 224.1]	-

The results reported in table X testify an improvement of our algorithm with respect to the dualMPC as well: TAR is reduced, as well as TDH, consequently TIR increases, precisely of 2.8% (on average) from the value achieved with the dualMPC. Moreover, this is achieved with a remarkably lower usage of insulin (TDI is smaller, on average). We observe a slightly minor TBR with the dual-action strategy, but with a statistically significant increase of the number of suggested hypotreatments, and so of the burden for the patient. These are promising results, considering also that the dualMPC is an already advanced technique, which, thanks to the planned hypotreatments, not only lowers the risk of hypoglycaemia but has the possibility to safely administer more basal insulin, as well.

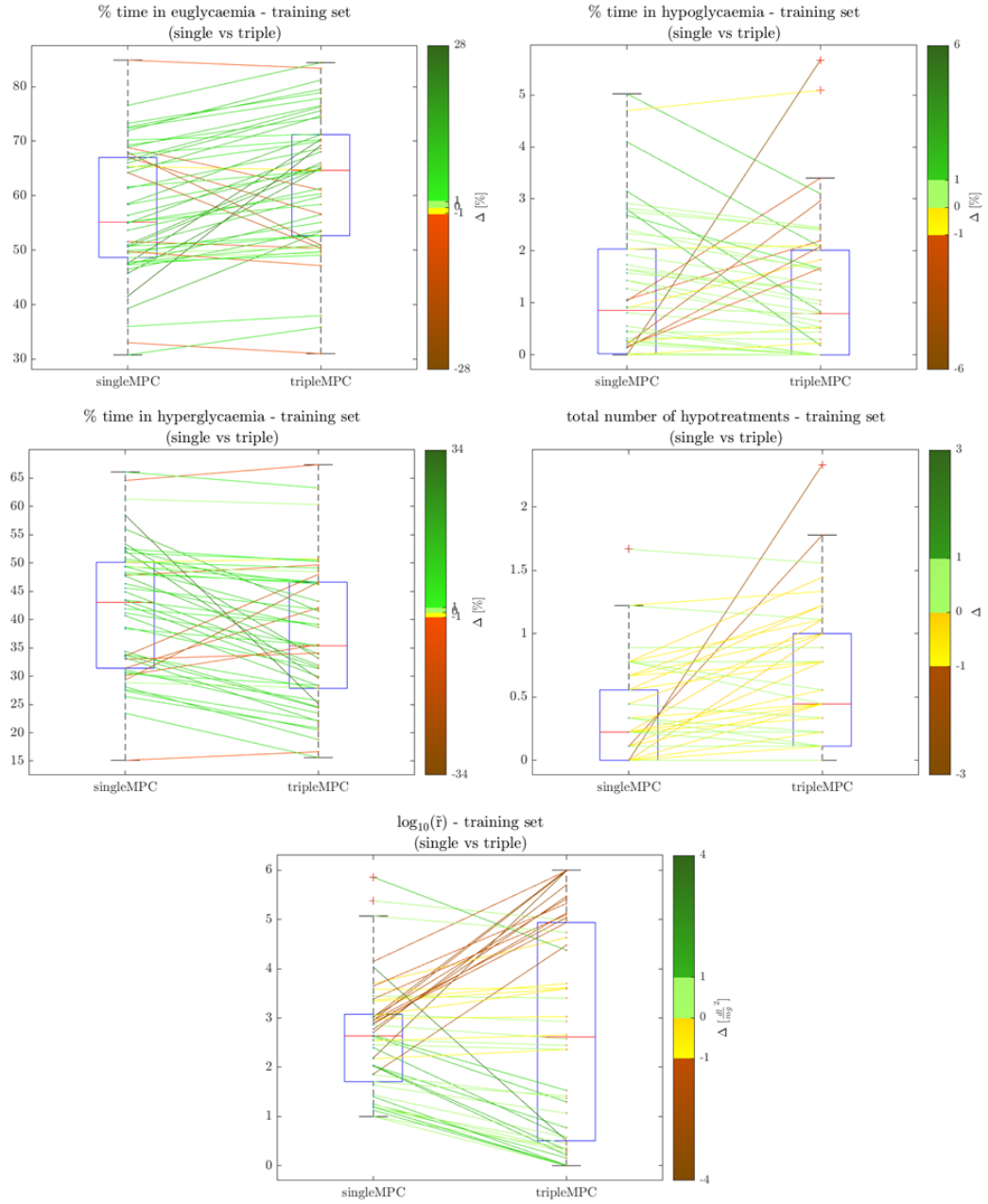

Figure 11. Boxplots, scatter plots and parallel coordinate plots for (from top to bottom, from left to right): TIR, TBR, TAR, n_{HT} and $log_{10}(\tilde{r})$, for the optimally tuned singleMPC and tripleMPC, in the advanced scenario. The logarithm is applied to $\tilde{r}$ to have a linear distribution.

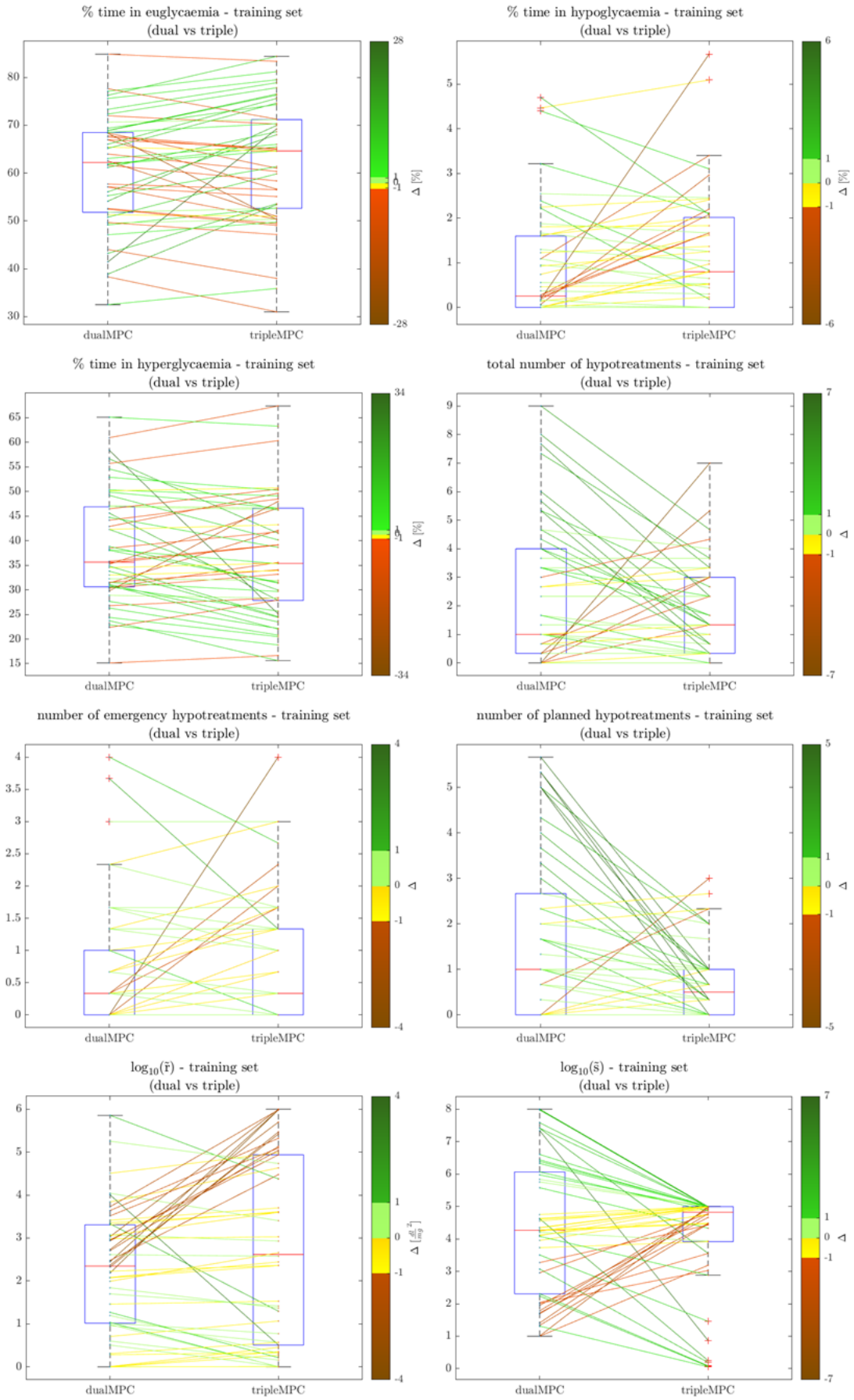

Figure 12. Boxplots, scatter plots and parallel coordinate plots for (from top to bottom, from left to right): TIR, TBR, TAR, n_{HT}, n_{eHT}, n_{pHT}, $log_{10}(\tilde{r})$ and $log_{10}(\tilde{s})$, for the optimally tuned dual- and tripleMPC (in the current scenario). The logarithm is applied to $\tilde{r}$ and $\tilde{s}$ to have a linear distribution.

Figures 11 and 12 show the boxplots, the scatter plot, and the parallel coordinate plot of the data regarding the fundamental metrics and the hyperparameters, collected for the three optimally tuned algorithms (in the robustness tests). We observe an improvement of the performances with the tripleMPC, specially with respect to the singleMPC, for most of the training set; this further supports the previous remarks, at an individual level as well.

Suboptimal tuning

Finally, we compare and discuss the results achieved with the three algorithms in the advanced scenario, on the testing set, therefore with the suboptimal parametrizations (inferred with the regression models).

testing set			
Variable	singleMPC	tripleMPC	p-value
μ_{CGM} $\left[\frac{\text{mg}}{\text{dl}}\right]$	$175.7\ [159.2 - 193.6]$	$168.7\ [158.4 - 186.5]$	0.2818
σ_{CGM} $\left[\frac{\text{mg}}{\text{dl}}\right]$	$59.9\ [47.5 - 72.6]$	$58.0\ [45.4 - 76.2]$	0.7981
$TIR^{\dagger}$ [%]	54.1 ± 15.2	56.7 ± 14.5	0.0031 *
TBR [%]	$1.4\ [0.0 - 3.2]$	$1.1\ [0.0 - 2.7]$	0.4640
$TAR^{\dagger}$ [%]	44.0 ± 14.8	41.2 ± 13.2	0.0010 *
TDh [%]	$0.0\ [0.0 - 1.2]$	$0.1\ [0.0 - 1.5]$	0.0254 *
TDH [%]	$10.5\ [2.2 - 21.2]$	$9.7\ [3.2 - 20.0]$	0.0754
AUC_h $\left[\frac{\text{min}*\text{mg}}{\text{dl}}\right]$	$423.8\ [0.0 - 1.6 \cdot 10^3]$	$351.9\ [0.0 - 1.9 \cdot 10^3]$	0.0630
${AUC_H}^{\dagger}$ $\left[\frac{\text{min}*\text{mg}}{\text{dl}}\right]$	$9.5 \cdot 10^4\ [5.2 \cdot 10^4 - 1.6 \cdot 10^5]$	$8.5 \cdot 10^4\ [4.9 \cdot 10^4 - 1.5 \cdot 10^5]$	0.1659
n_{HT}	$0.3\ [0.0 - 0.7]$	$0.7\ [0.4 - 1.2]$	$1.1 \cdot 10^{-7}$ *
n_{eHT}	-	$0.2\ [0.0 - 0.8]$	-
n_{pHT}	-	$0.4\ [0.3 - 0.7]$	-
q_{HT} [g]	$4.2\ [0.0 - 12.2]$	$11.9\ [7.2 - 24.4]$	$6.2 \cdot 10^{-8}$ *
q_{eHT} [g]	-	$3.3\ [0.0 - 15.0]$	-
q_{pHT} [g]	-	$8.1\ [5.0 - 11.7]$	-
${n_{bol}}^{\dagger}$	-	4.3 ± 1.9	-
q_{bol} [U]	-	$5.7\ [3.8 - 9.6]$	-
$TDI^{\dagger}$ [U]	44.4 ± 11.1	41.0 ± 12.2	$8.2 \cdot 10^{-10}$ *
$\tilde{r}$ $\left[\left(\frac{\frac{\text{kg}}{\text{min}}}{\text{pmol}}\right)^2\right]$	$400.1\ [164.8 - 888.8]$	$537.4\ [108.4 - 2.3 \cdot 10^3]$	$6.7 \cdot 10^{-4}$ *
$\tilde{s}^{\dagger}$	-	$1.1 \cdot 10^4 \pm 1.9 \cdot 10^3$	-
$\widetilde{w}_1$ $\left[\left(\frac{\frac{\text{kg}}{\text{min}}}{\text{pmol}}\right)^2\right]$	-	$0.3\ [0.1 - 0.7]$	-
${\widetilde{w}_2}^{\dagger}$	-	30.5 ± 0.1	-

Table XI (above) and XII (below). Metrics and hyperparameters for the sub-optimally tuned singleMPC (table XI), dualMPC (table XII) and tripleMPC, in the advanced scenario. For the variables which are normally distributed (symbol †), the mean ± the standard deviation is reported, while for the others the median and the interquartile range ([$25^{th} - 75^{th}$ percentile]). The variables that differ in a statistically significant way are identified by the symbol *, beside the p-value resultant from the relative statistical test.

testing set			
Variable	dualMPC	tripleMPC	p-value
μ_{CGM} $\left[\frac{\text{mg}}{\text{dl}}\right]$	172.1 [156.3 − 188.5]	168.7 [158.4 − 186.5]	0.0703
σ_{CGM} $\left[\frac{\text{mg}}{\text{dl}}\right]$	57.4 [44.9 − 72.4]	58.0 [45.4 − 76.2]	0.0529
$TIR^{\dagger}$ [%]	56.2 ± 16.5	56.7 ± 14.5	0.5373
TBR [%]	1.2 [0.0 − 3.1]	1.1 [0.0 − 2.7]	0.6207
$TAR^{\dagger}$ [%]	41.8 ± 15.5	41.2 ± 13.2	0.4509
TDh [%]	0.0 [0.0 − 1.0]	0.1 [0.0 − 1.5]	0.0044 *
TDH [%]	10.3 [1.5 − 20.1]	9.7 [3.2 − 20.0]	0.9352
AUC_h $\left[\frac{\text{min}*\text{mg}}{\text{dl}}\right]$	305.2 [0.0 − $1.7 \cdot 10^3$]	351.9 [0.0 − $1.9 \cdot 10^3$]	0.0161 *
$AUC_H{}^{\dagger}$ $\left[\frac{\text{min}*\text{mg}}{\text{dl}}\right]$	$8.6 \cdot 10^4$ [$3.8 \cdot 10^4$ − $1.5 \cdot 10^5$]	$8.5 \cdot 10^4$ [$4.9 \cdot 10^4$ − $1.5 \cdot 10^5$]	0.7437
n_{HT}	0.2 [0.1 − 0.3]	0.7 [0.4 − 1.2]	0.0038 *
n_{eHT}	0.1 [0.0 − 0.3]	0.2 [0.0 − 0.8]	0.1107
n_{pHT}	0.0 [0.0 − 0.2]	0.4 [0.3 − 0.7]	0.0048 *
q_{HT} [g]	2.4 [1.1 − 5.2]	11.9 [7.2 − 24.4]	$2.8 \cdot 10^{-6}$ *
q_{eHT} [g]	1.6 [0.0 − 4.4]	3.3 [0.0 − 15.0]	0.0277 *
q_{pHT} [g]	0.4 [0.0 − 1.9]	8.1 [5.0 − 11.7]	$2.7 \cdot 10^{-7}$ *
$n_{bol}{}^{\dagger}$	-	4.3 ± 1.9	-
q_{bol} [U]	-	5.7 [3.8 − 9.6]	-
$TDI^{\dagger}$ [U]	46.0 ± 12.6	41.0 ± 12.2	$8.0 \cdot 10^{-21}$ *
$\tilde{r}$ $\left[\left(\frac{\frac{\text{kg}}{\text{min}}}{\text{pmol}}\right)^2\right]$	149.8 [49.9 − 519.4]	537.4 [108.4 − $2.3 \cdot 10^3$]	$1.8 \cdot 10^{-9}$ *
$\tilde{s}^{\dagger}$	$2.8 \cdot 10^4$ [$8.2 \cdot 10^3$ − $1.2 \cdot 10^5$]	$1.1 \cdot 10^4 \pm 1.9 \cdot 10^3$	$1.4 \cdot 10^{-5}$ *
$\widetilde{w}_1$ $\left[\left(\frac{\frac{\text{kg}}{\text{min}}}{\text{pmol}}\right)^2\right]$	-	0.3 [0.1 − 0.7]	-
$\widetilde{w}_2{}^{\dagger}$	-	30.5 ± 0.1	-

As for the values observed with the suboptimal tuning, in the original scenario, there is a degradation of the performances for each algorithm, but more evidently for the tripleMPC. For instance, the average TIR decreases of 5.5 units for the tripleMPC, while it lowers of 2.9 units for the singleMPC and 4.3 units for the dualMPC, with respect to the case with the optimal tuning. This is due to the expected approximation error of the regression models, which is likely major for the regression law of $\widetilde{w}_2$. Nonetheless, our technique still performs significantly better with respect to the single-action approach: there is a statistically significant decrease of TAR,

so an increase of TIR (of 4.8% on average), in addition with a significantly lower usage of insulin. We notice an increment of TDh, probably because the suboptimal hyperparameters that determine the boluses' administration lead to an aggressive administration, and of the extra-CHO as well, which is expected. The remarks regarding TIR and TAR are valid at an individual level as well, basing on figure 13, where we notice particularly a lowering of the time-above-range, and thus an increment of the time-in-range, for many of the patients of the testing set.

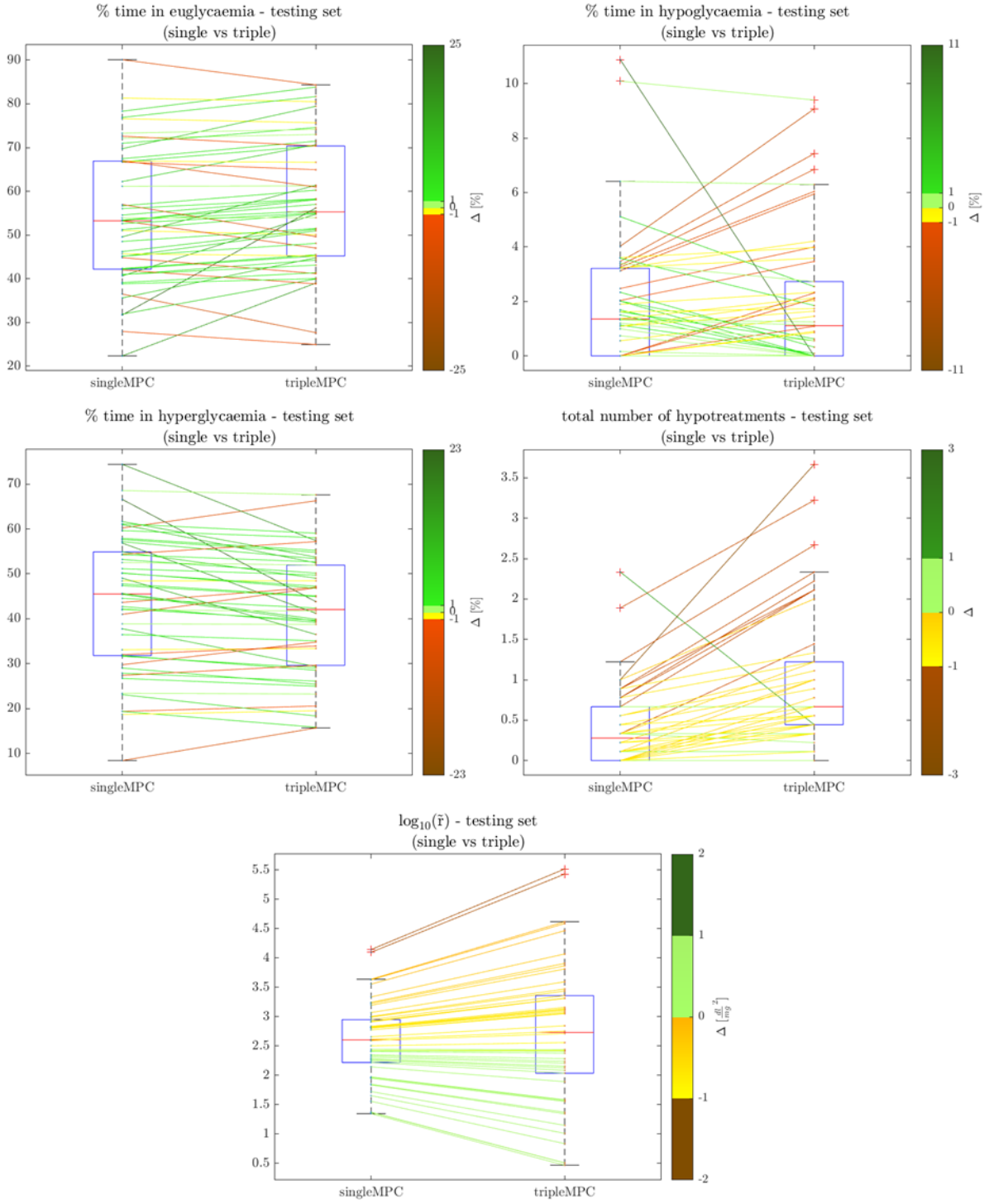

Figure 13. Boxplots, scatter plots and parallel coordinate plots for (from top to bottom, from left to right): TIR, TBR, TAR, n_{HT} and $log_{10}(\tilde{r})$, for the sub-optimally tuned singleMPC and tripleMPC, in the advanced scenario.

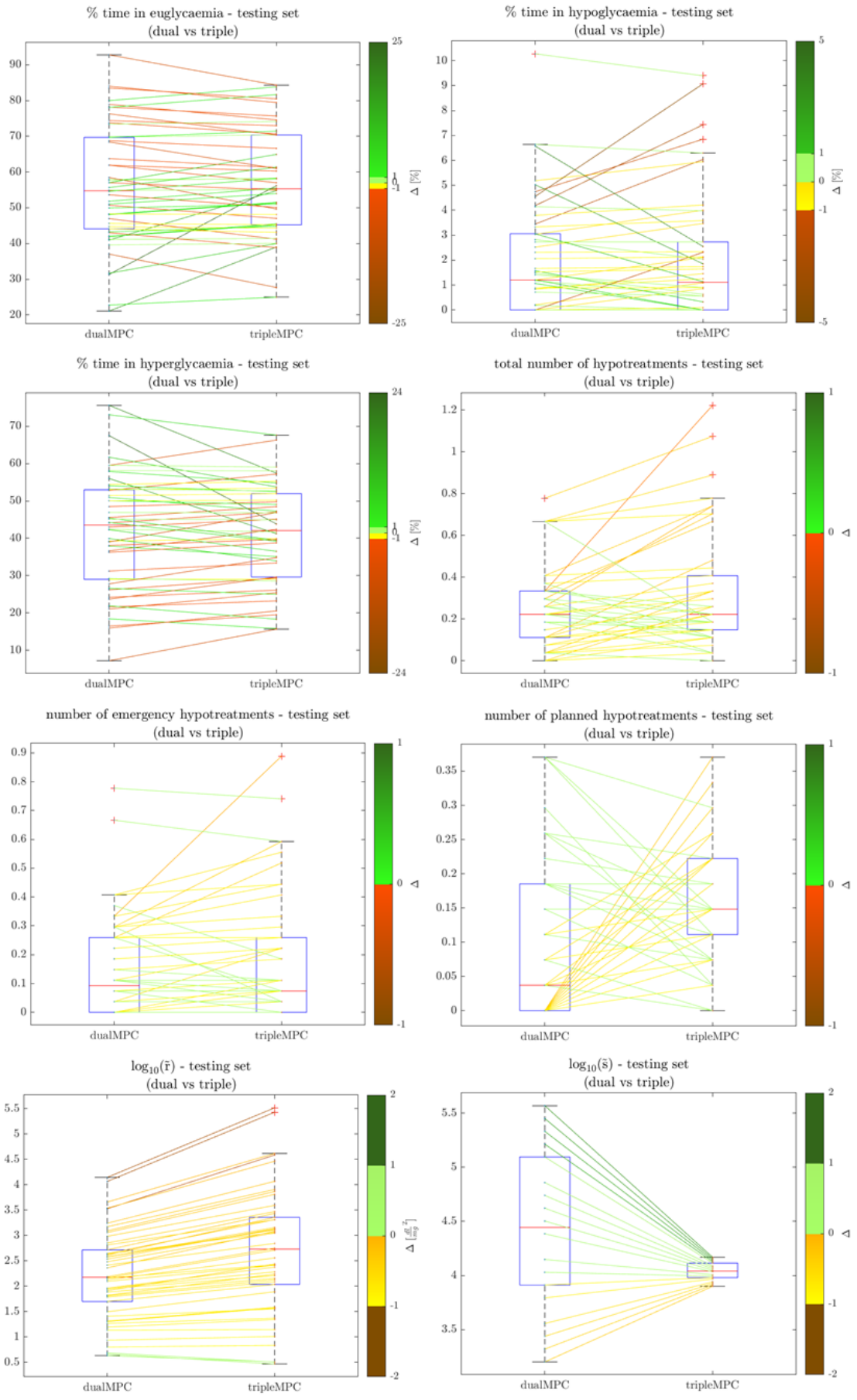

Figure 14. Boxplots, scatter plots and parallel coordinate plots for (from top to bottom, from left to right): TIR, TBR, TAR, n_{HT}, n_{eHT}, n_{pHT}, $log_{10}(\tilde{r})$ and $log_{10}(\tilde{s})$, for the dual- and the tripleMPC (in the advanced scenario), with suboptimal tuning.

We notice a lowering of TAR and thus an increment of TIR also with respect to the dualMPC, even if in this case these differences are not statistically significant. With the tripleMPC, there is an increase of TDh and the hypotreatments, as well. Overall, the performances of our algorithm and the dual-action strategy, with a suboptimal parametrization, are almost comparable. Considering the limited quality of the regression models (particularly for $\widetilde{w}_2$) and the fact that the dualMPC is already an advanced technique, these results are decorous. The individual results concerning some fundamental metrics (and the hyperparameters) are shown in figure 14, and confirm the previous statement.

In conclusion, the overall outcomes of the tests performed in the advanced scenario confirm that this is much more appropriate to test the capabilities of the tripleMPC, and prove the real usefulness and the positive impact on control of the corrective boluses, in such a scenario which is possibly more realistic, as well. In this scenario, our algorithm is proven to outperform both a state-of-the-art strategy (i.e., the singleMPC) and an advanced approach (the dualMPC), with the optimal parametrization, thanks exactly to the additional capability to plan the administration of the extra boluses, coupled with the planning of hypotreatments and the basal insulin modulation. Adopting a suboptimal tuning, inferred by using regression models (which, in addition, can be improved), the tripleMPC still outperforms the singleMPC, and shows almost comparable performances with respect to the dualMPC, with a slightly lower time-above-range and thus a major time-in-range.

VI. Conclusions

The core of this thesis project is the development of the triple-action MPC AP (or tripleMPC), an algorithm for the inclusion in an AP of the capability to proactively plan the suggestion of CHO intakes to the patient and the administration of corrective insulin boluses, together with the basal insulin modulation. The idea is to reinforce the counteraction of hypo- and hyperglycaemia, respectively. This is done by using MPC, a model-based predictive strategy, which formulates the control problem as an optimization one, and allows to impose constraints on the control variables. This is achieved by starting and taking inspiration from the work of Pavan et al. in [17], where an approach to introduce the CHO suggestions is proposed. The suggestible CHO amount is modelled as a quantized variable c, by including in the control problem two Boolean support variables c_1 and c_2, thus reconducting the optimization to a MIQP problem; in addition, a series of constraints are imposed on these Boolean variables, in order to impose the sparsity in time of the suggestions, to limit their daily number and to forbid their use in predefined periods of the day ("do-not-disturb" zones). All this is needed to contain the burden of the patient, which must manually assume the suggested CHO doses. Conversely, the amount of a corrective bolus is represented by a continuous variable b; together with the fact that the boluses are early planned in synergy with the other control variables, this makes our approach innovative with respect to the state-of-the-art strategies. An additional Boolean support variable z is included, to model the capability of the algorithm to choose whether to deliver a bolus or not, and to impose the sparsity in time on the boluses as well, by imposing suitable constraints on z.

Our algorithm is compared to a state-of-the-art strategy, the single-action MPC AP (in short, singleMPC), which only modulates the basal insulin infusion, and the advanced technique proposed by Pavan et al. in [17] (the dual-action MPC AP or, in brief, dualMPC), with the additional capability to plan CHO suggestions. The assessment of the performances of the three algorithms is performed via *in-silico* trials, by exploiting the *UVa/Padova T1D Simulator* (v. 2013), an accurate model of the metabolic subsystem of a T1D patient, which was approved by FDA as a substitute of animal testing for preclinical trials for T1D therapies evaluation. The model's parameters are not fixed, conversely the simulator is associated to a dataset of 100 virtual adult patients, each one being a different realistic parameters' set, to perform the trials on. The model our MPC is based on is a linearized version exactly of the *UVa/Padova T1D* system of the average virtual subject.

The basic simulation scenario that we consider covers three days, each one including the consumption of three meals, and is characterized by realistic features. However, it turns out to be limiting to evaluate the actual potential of the tripleMPC; therefore, we consider a more suitable alternative scenario as well, where an unannounced persistent hyperglycaemic event is added, during each simulated night. Even if the generation mechanism of these hyperglycaemias is not properly realistic, this makes sense, since the real hyperglycaemic events are persistent as well, and can occur due to other disturbing factors, apart from meals.

There is a subset of our MPC's hyperparameters (i.e., the weights in the MPC's cost function) which have to be individualized, due to the high inter-subject biovariability. The search of the optimal patient-specific tuning must be performed via trial-and-error, i.e. testing different combinations of the parameters (in our work, chosen basing on a Bayesian approach) and selecting the one associated to the best performances. This would be dangerous and thus cannot be done for any real patient; therefore, basing on the optimal values obtained for a training set of subjects, a regression law is retrieved for each hyperparameter, to be used for any T1D individual to estimate the best tuning for him or her. The quality of these regression models is assessed on a testing set.

The overall results confirm that the advanced scenario (i.e., with the additional persistent hyperglycaemias) is more appropriate to test the real potential of our strategy, and show how it can outperform both the state-of-the-art approach (the single-action MPC AP) and the advanced one (the dual-action MPC AP), with the optimal tuning of the hyperparameters. Indeed, in this case, we notice an increase of the average time-in-range of more than 9%, with respect to the former, and almost 3%, with respect to the latter. Adopting a suboptimal parametrization, inferred by using the regression laws, we assist to a degradation of the performances for each algorithm, but which is more evident for the tripleMPC; therefore, the need to improve the regression models emerges. Nonetheless, also in this case our approach outperforms the single-action technique, with an increment of the time-in-range of almost 5% on average, while it shows comparable performances with respect to the dual-action MPC AP, with a slight lowering of the time-above-range and a correspondent increase of the time-in-range. In conclusion, these results are appreciable and promising, demonstrating the usefulness and the positive impact on control of the administration of early-planned corrective boluses, being coupled with the basal insulin modulation and the suggestion of scheduled hypotreatments.

6.1. Future developments

There is a series of possible future improvements for our algorithm.

First, the generation mechanism of the persistent hyperglycaemias, that we introduced in the advanced simulation scenario (i.e., for the robustness test), must be improved such to be more realistic. Indeed, it is rough and is not based on any real observations of this phenomenon. Therefore, this upgrade could be achieved by referring to and exploiting real data.

In addition, PH could be increased, so that the MPC can predict in a more complete and therefore better way the effects of a planned bolus. However, in this way the number of optimization variables increases and the simulation times can become too much large, making the execution of all the needed tests particularly onerous. A solution to increase PH, but limiting this problem, consists in computing only the optimal sequence of control actions from the current time k to $k + PH_i$, with PH_i (Input or Control Horizon) smaller than PH (Output or Prediction Horizon), while forcing the control variables to be constant for the remaining period of the Prediction Horizon, e.g. equal to the values computed for the time $k + PH_i$. This can be done because the assumption holds that the elements of the optimal sequence after a certain PH_i have less impact on the value calculated for the control actions at the current time. Consequently, the number of variables to be computed decreases, as well as the computational time.

Moreover, the model the MPC relies on could be modified introducing a nonlinearity, to better describe the pharmacodynamics of insulin, in particular to highlight the insulin resistance that is found in hyperglycaemia. In this way, the controller could better predict the actual advantages of boluses with respect to the basal insulin. For instance, this could be done by describing with a Hill function the relation between the quantity of the administered insulin with its effect on glycaemia, so that the latter is significantly larger over an insulin threshold amount, that only a bolus can overcome [30]. However, this would complicate the problem and might increase the computational cost, requiring to resort to a nonlinear MPC including the optimization of Boolean variables.

Furthermore, a development for the near future could be to use glucagon (the antagonist hormone of insulin) instead of CHO. This would make the system fully automatic and thus it would lower the burden on the patient, since glucagon can be administered subcutaneously with a pump of its own, as well as insulin. This is an option that is currently being explored [31-32]; however, there is still no full consensus on the long-term safety of glucagon and so on whether it could be securely included as a true additional control variable or if it should be used only as

mere emergency measure. This is mostly due to the fact that the hepatic extraction[13] mechanism, which is stimulated by glucagon, may fail in case of depleted glycogen storage or may be inhibited by substances such as alcohol [17].

Finally, there is a declination of the tripleMPC of practical relevance and that may be worth to be explored, that is a system for the proactive planning only of CHO intakes and insulin boluses' (manual) administrations (without the automated basal insulin modulation). De facto, this is a Decision Support System (DSS) for the early suggestion of hypo- and hypertreatments. This should be thought as coupled with a manual therapy and so, potentially, it could apply not necessarily only to an AP-like architecture: indeed, in this case where the boluses' delivery can be performed without resorting to an insulin pump (that is no longer indispensable), but e.g. via insulin pen, only a CGM sensor is needed. The resultant architecture is simpler and, specially, pump-faults-free, therefore the advantage is that it could be manageable also by those patients that are less capable and expert. In order to calm the risk of bolus-amount-counting errors and to limit the burden on the patient, the boluses should be respectively quantized and constrained to be sparse in time as well.

[13] The release in blood of glucose stored in the liver, in form of glycogen.

Appendices

A.1. Notation

In this appendix we report a few details on the notation we resort to.

ℓ_2-norm

In the cost functions (3), (14) and (27) a notation like $\|v(k)\|_W^2$ is adopted. This stands for the ℓ_2-norm and corresponds to

$$\|v(k)\|_W^2 = v(k)^T W v(k) \quad (A1)$$

where $v \in R^{n\times 1}$ is a vector and $W \in R^{n\times n}$ is a weight matrix.

ℓ_0-norm

In (14) and (27), the weighted sum of the squares of the Boolean variables c_1 and c_2, for each time step within a given prediction horizon, is included, that is

$$\sum_{j=1}^{PH-1} \tilde{s}(c_1(k+j)^2 + c_2(k+j)^2) = \sum_{j=1}^{PH-1} \tilde{s}\big(c_1(k+j) + c_2(k+j)\big)$$
$$= \sum_{j=1}^{PH-1} \tilde{s} \cdot c_{bool}(k+j)\,. \quad (A2)$$

The signal $c_{bool}(\cdot)$, i.e. comprehending every $c_{bool}(k+j)\ \forall k,j$, is dichotomic as well. It is non-null when $c_1(k)$ or $c_2(k)$ is active, i.e. whenever $c(k) = \gamma_1 \cdot c_1(k) + \gamma_2 \cdot c_2(k) \neq 0$; in other words, it takes into account the number of times a CHO intake is suggested, regardless the amount. This is the so-called ℓ_0-norm.

A.2. Basal insulin reference

As discussed in section 2.1, the reference signal for the control variable $\bar{\iota}$ is defined as in [24]:

$$i_{meal}(k) = \begin{cases} \dfrac{\hat{d}(k)}{CR} + \dfrac{g(k) - G_b}{CF} - IOB(k) & at\ meal\ times \\ 0 & otherwise \end{cases},$$

that is the heuristic formula for the meal boluses' calculation, coming from the traditional therapy. The carbohydrates-to-insulin ratio CR is the amount of CHO covered by 1 U of insulin,

therefore the first term $\frac{\hat{d}(k)}{CR}$ is the quantity of insulin that is expected to balance the CHO content of the announced meal. CF represents the glycaemic drop caused by 1 U of insulin; consequently, $\frac{g(k)-G_b}{CF}$ is a correction term that takes into account the distance, with sign, of the current measurement of $g(k)$ from the patient's basal glycaemia G_b, and it is an additional amount of insulin, if positive, or a quantity to be subtracted, if $g(k) < G_b$. The last term $IOB(k)$ is the so-called insulin-on-board, namely how much insulin is still active in the body at the considered time. It can be estimated as reported in [5], i.e. by giving the currently infused insulin dose to the state-space model

$$\begin{cases} x(k+1) = \begin{bmatrix} -13 \cdot 10^{-3} & 0 \\ 13 \cdot 10^{-3} & -13 \cdot 10^{-3} \end{bmatrix} x(k) + \begin{bmatrix} 1 \\ 0 \end{bmatrix} i(k) \\ y(k) = [1 \quad 1] x(k) \end{cases}, \quad (A3)$$

then rounding to the second decimal place and applying a delay of one sampling time to the resultant output $y(k)$.

A.3. QP and MIQP problems' formulation

An optimization problem can be reconducted to a (MI)QP formulation like

$$\min_{\substack{x \ s.t. \\ Ax-b \leq 0}} \frac{1}{2} x^T Q x + c^T x,$$

where x is the optimization variable, Q a positive definite matrix and c a vector, if the adopted model is linear, the cost function is quadratic, and the constraints can be expressed in the linear form $Ax - b \leq 0$. This can be done for each considered algorithm, since in each case the respective optimization problem is compliant to these assumptions. This is convenient, because in this way it is assured that the problem is convex (so no local minima exist and the convergence is guaranteed) and there are efficient and steady algorithms for its resolution (e.g. Interior-Point, Active Set).

To do this, the following lemma is needed.

Lemma. $\sum_{j=1}^{N} w \cdot v(k+j)^2 = V(k)^T W V(k) \ \forall k$, with $V(k) = [v(k), \dots, v(k+N)]^T \in R^{N \times 1}$, $W = \begin{bmatrix} w & 0 & \dots & 0 \\ 0 & \ddots & & \vdots \\ \vdots & & \ddots & 0 \\ 0 & \dots & 0 & w \end{bmatrix} \in R^{N \times N}$, $v(k)$ a scalar variable and $w \in R$.

Proof. $V(k)^T W V(k) = V(k)^T \cdot wI \cdot V(k) = v(k) \cdot w \cdot v(k) + \cdots + v(k+N) \cdot w \cdot v(k+N) = w \cdot v(k)^2 + \cdots + w \cdot v(k+N)^2 = \sum_{j=1}^{N} w \cdot v(k+j)^2$.

The QP formulation of the singleMPC optimization problem in (9) is achieved by defining $U(k)$, F_s, f_s as shown in section 2.1 and manipulating the cost function (3) as follows.

$$\tilde{J} = \sum_{j=0}^{PH-1} \left(\left(\bar{g}(k+j) - \overline{g_0}(k+j) \right)^2 + \tilde{r} \left(\bar{\imath}(k+j) - \overline{\imath_0}(k+j) \right)^2 \right) + \|\bar{x}(k+PH)\|_P^2 =$$

$$= \sum_{j=1}^{PH-1} \left(\left(\bar{g}(k+j) - \overline{g_0}(k+j) \right)^2 \right) + \sum_{j=0}^{PH-1} \left(\tilde{r} \left(\bar{\imath}(k+j) - \overline{\imath_0}(k+j) \right)^2 \right) + \|\bar{x}(k+PH)\|_P^2$$

since the output at the current time k depends on the control action at $k-1$, which is not included in the current prediction horizon. Moreover, for the lemma reported above:

$$\tilde{J} = (Y(k) - Y_0(k))^T Q (Y(k) - Y_0(k)) + (U(k) - U_0(k))^T R (U(k) - U_0(k)) \quad (A4)$$

with

$$Y(k) = [\bar{g}(k+1), \dots, \bar{g}(k+PH-1), \bar{x}(k+PH)^T]^T \in R^{PH+15 \times 1},$$

$$U(k) = [\bar{\imath}(k), \dots, \bar{\imath}(k+PH-1)] \in R^{PH \times 1},$$

$$Q = \begin{bmatrix} 1 & 0 & \dots & 0 \\ 0 & \ddots & & \vdots \\ \vdots & & 1 & 0 \\ 0 & \dots & 0 & P \end{bmatrix} \in R^{PH+15 \times PH+15}, \quad R = \begin{bmatrix} \tilde{r} & 0 & \dots & 0 \\ 0 & \ddots & & \vdots \\ \vdots & & \ddots & 0 \\ 0 & \dots & 0 & \tilde{r} \end{bmatrix} \in R^{PH \times PH}.$$

Given the model (1), the prediction of the output evolution, for a generic N, can be computed at a given time k by solving the equation:

$$\bar{g}(k+N|k) = CA^N \bar{x}(k|k) + \sum_{j=1}^{N} CA^{N-j} B \bar{\imath}(k+j-1|k). \quad (A5)$$

Therefore,

$$Y(k) = \tilde{A}_C \bar{x}(k) + \tilde{B}_C U(k) + \tilde{M}_C D(k) \quad (A6)$$

with

$$\tilde{A}_C = \tilde{C}\tilde{A}, \quad \tilde{B}_C = \tilde{C}\tilde{B}, \quad \tilde{M}_C = \tilde{C}\tilde{M},$$

$$\tilde{C} = \begin{bmatrix} C & 0 & \dots & 0 \\ 0 & \ddots & & \vdots \\ \vdots & & C & \vdots \\ 0 & \dots & \dots & 0 \end{bmatrix} \in R^{PH+15\times 16PH}, \quad \tilde{A} = \begin{bmatrix} A \\ A^2 \\ \vdots \\ A^{PH} \end{bmatrix} \in R^{16PH\times 16},$$

$$\tilde{B} = \begin{bmatrix} B & 0 & \dots & \dots & \dots & 0 \\ AB & B & 0 & \dots & \dots & \vdots \\ A^2B & AB & B & 0 & \dots & 0 \\ \vdots & \vdots & \vdots & \vdots & \vdots & \vdots \\ \vdots & \vdots & \vdots & \vdots & \vdots & 0 \\ A^{PH-1}B & A^{PH-2}B & \dots & \dots & AB & B \end{bmatrix} \in R^{16PH\times PH},$$

$$\widetilde{M} = \begin{bmatrix} M & 0 & \dots & \dots & \dots & 0 \\ AM & M & 0 & \dots & \dots & \vdots \\ A^2M & AM & M & 0 & \dots & 0 \\ \vdots & \vdots & \vdots & \vdots & \vdots & \vdots \\ \vdots & \vdots & \vdots & \vdots & \vdots & 0 \\ A^{PH-1}M & A^{PH-2}M & \dots & \dots & AM & M \end{bmatrix} \in R^{16PH\times PH},$$

$$D(k) = \begin{bmatrix} \hat{d}(k) \\ \vdots \\ \hat{d}(k+PH-1) \end{bmatrix} \in R^{PH\times 1}.$$

Consequently,

$$\begin{aligned} \tilde{J} = &\left(\tilde{A}_C\bar{x}(k) + \tilde{B}_C U(k) + \widetilde{M}_C D(k) - Y_0(k)\right)^T Q\left(\tilde{A}_C\bar{x}(k) + \tilde{B}_C U(k) + \widetilde{M}_C D(k) - Y_0(k)\right) \\ &+ \left(U(k) - U_0(k)\right)^T R\left(U(k) - U_0(k)\right) = \\ = &\left(\tilde{A}_C\bar{x}(k) + \widetilde{M}_C D(k) - Y_0(k)\right)^T Q\left(\tilde{A}_C\bar{x}(k) + \widetilde{M}_C D(k) - Y_0(k)\right) + U_0(k)^T R U_0(k) \\ &+ \left(\tilde{A}_C\bar{x}(k) + \widetilde{M}_C D(k) - Y_0(k)\right)^T Q\left(\tilde{B}_C U(k)\right) \\ &+ \left(\tilde{B}_C U(k)\right)^T Q\left(\tilde{A}_C\bar{x}(k) + \widetilde{M}_C D(k) - Y_0(k)\right) - U_0(k)^T R U(k) \\ &- U(k)^T R U_0(k) + U(k)^T\left(B_C{}^T Q B_C + R\right)U(k). \qquad (A7) \end{aligned}$$

Notice that the first two terms in the second expression in (A7) are constant with respect to the optimization variable $U(k)$ and so can be discarded; in addition, the third term is equal to its transposed that is equal to the fourth term, and analogously for the fifth and the sixth terms. Therefore,

$$\begin{aligned} \tilde{J} = 2&\left(\left(\tilde{A}_C\bar{x}(k) + \widetilde{M}_C D(k) - Y_0(k)\right)^T Q\tilde{B}_C - U_0(k)^T R\right)U(k) \\ &+ U(k)^T\left(B_C{}^T Q B_C + R\right)U(k). \qquad (A8) \end{aligned}$$

Since $\tilde{J}$ has to be minimized, multiplicative terms do not count and so it can be divided by 2, thus obtaining an equivalent cost function:

$$\tilde{J}' = \frac{1}{2} U(k)^T Q_s U(k) + c_s^T U(k) \quad (A9)$$

that is the QP formulation of $\tilde{J}$ for the singleMPC, with

$$Q_s = {B_C}^T Q B_C + R,$$
$$c_s = \left(\left(\tilde{A}_C \bar{x}(k) + \tilde{M}_C D(k) - Y_0(k) \right)^T Q \tilde{B}_C - U_0(k)^T R \right)^T . \quad (A10)$$

The MIQP formulation of the optimization problems of the dual- and the tripleMPC, in (21) and (34) respectively, can be obtained defining F_d, f_d, F_t, f_t as shown in sections 2.2 and 2.3, and performing analogous manipulations. The main difference is that $U(k)$ has to be redefined, in each case, as reported in the same sections, and $\tilde{B}$ has to be substituted with

$$\tilde{B}' = [\tilde{B} \quad \gamma_1 \widetilde{M} \quad \gamma_2 \widetilde{M}] \in R^{16PH \times 3PH} \quad (A11)$$

for the dualMPC, and with

$$\tilde{B}'' = [\tilde{B} \quad \gamma_1 \widetilde{M} \quad \gamma_2 \widetilde{M} \quad \tilde{B} \quad 0] \in R^{16PH \times 5PH} \quad (A12)$$

for the tripleMPC. Notice that the last block of $\tilde{B}''$ is null, since it multiplies the vector $Z(k) = [z(k) \quad \dots \quad z(k + PH - 1)]^T$, which is not included in the model.

A.4. Carb-counting-error and emergency hypotreatments

In the adopted simulation scenario, there is also a patient decisions' model [22], which is needed to simulate the meal announcement mechanism, in particular the carb-counting-error (CCE) committed by the patient and affecting the meal's CHO amount reported to the system, and the emergency hypotreatments (eHT) generation process. In this appendix, we discuss how the CCE is modelled and how the eHT originate.

Carb-counting-error

To simulate the estimated CHO amount of an announced meal, a model of the probability density function of the carb-counting-error is involved. This model is a non-standardized Student's t function, and it is fitted by maximum-likelihood to the data published by Brazeau et al. in [33], in which the CHO content of 448 meals was estimated by T1D patients and in parallel assessed by a dietitian [22].

Emergency hypotreatments

In the scenario we consider, self-monitoring blood glucose (SMBG) measurements are included as well, namely additional checks of the blood glucose (BG), manually performed by the patient in parallel with CGM readings. SMBG checks are involved to monitor hypoglycaemia; indeed, they are triggered in response to hypoglycaemia symptoms, which are generated when the BG level falls below a patient-specific threshold of hypoglycaemia awareness, or if the CGM measurement goes below $70\ \frac{\text{mg}}{\text{dl}}$ (the patient-independent threshold of hypoglycaemia) and if at least 15 min are passed since the last SMBG check and CHO intake [22]. In other words, SMBG measurements are triggered whenever the measured BG is close to or below $70\ \frac{\text{mg}}{\text{dl}}$.

An emergency hypotreatment is generated after a SMBG check for hypoglycaemia, if the measured BG is below $70\ \frac{\text{mg}}{\text{dl}}$. During waking hours ($06{:}00\ \text{AM} - 10{:}00\ \text{PM}$), the amount of the hypotreatment is set to 15 g if SMBG $> 55\frac{\text{mg}}{\text{dl}}$ or 20 g if SMBG $\leq 55\frac{\text{mg}}{\text{dl}}$. After 15 min, a re-check for hypoglycaemia is simulated, with a probability of 10%; if at the re-check the SMBG measurement is still below $70\frac{\text{mg}}{\text{dl}}$, another hypotreatment is given. Conversely, during night hours ($10{:}00\ \text{PM} - 06{:}00\ \text{AM}$), the hypotreatments' amount is set to 25 g, whatever the entity of the detected hypoglycaemic event, and no re-checks for hypoglycaemia are simulated. Finally, any hypotreatment is assumed to be consumed in one minute [22].

A.5. Stepwise regression

To perform the regressors' selection procedure, presented in section IV, we resort to the stepwise regression algorithm. The idea it is based on is to proceed by steps, considering one variable at a time and including it in the regression model only if it respects the criterion chosen to quantify the model fit to the data.

There are more variants of this technique. The forward selection approach involves starting with an empty pool of regressors, and adding a variable if its inclusion improves the fit in statistically significant way. Conversely, with the backward elimination variant, the initial set of regressors includes all the candidate variables, and each one is dismissed from the model only if its loss does not deteriorate the model fit, in a statistically significant way. In this case, we employ the bidirectional elimination approach, that is the combination of the two above: first, the forward selection is used, then the backward elimination is applied to the regressors' set resultant from the previous phase.

There are more selection criterions as well, to evaluate in different ways the model fit, and so to decide if the model at a given step is better than the one at the previous step or not; we limit to presenting only the two principles used in our work. First, the Sum of Squared Errors (SSE) criterion, which consists in computing, at each step, exactly the sum of squares of the differences between the observed data and the values predicted with the current model; if the new SSE is lower than the SSE from the previous step, the variable which is currently considered is included in the model. To evaluate if the SSE lowering is statistically significant, a F-test (also known as ANOVA test) is performed. Conversely, the Akaike Information Criterion (AIC) involves the calculation (at each step) of the AIC value, defined as:

$$AIC = 2k - 2\ln(\hat{L}) \quad (A13)$$

where k is the number of variables in the present model, and $\hat{L}$ the maximum value of the likelihood function associated to the model (i.e., the probability density function of the observed data, as a function of the current model's regressors). The lower the AIC value, the better the model, since in this way there is a trade-off between the minimization of the number of regressors k and the maximization of the quality of the model, quantified by $\hat{L}$. When using the forward selection, the improvement of the model fit at a given step is statistically significant if the decrease of AIC is lower than a maximum threshold; in the backward elimination approach, the worsening of the model quality is statistically significant if the AIC value's increase is larger than a minimum threshold.

References

[1] L. A. DiMeglio, C. Evans-Molina and R. A. Oram, *"Type 1 diabetes"*, The Lancet, vol. 391, n. 10138, pp. 2449-2462, 2018.

[2] C. Cobelli, C. Dalla Man, G. Sparacino, L. Magni, G. De Nicolao and B. P. Kovatchev, *"Diabetes: models, signals, and control"*, IEEE reviews in biomedical engineering, vol. 2, pp. 54-96, 2009.

[3] A. Bertachi, C. M. Ramkissoon, J. Bondia and J. Vehí, *"Automated blood glucose control in type 1 diabetes: A review of progress and challenges"*, Endocrinología, Diabetes y Nutrición (English ed.), vol. 65, n. 3, pp. 172-181, 2018.

[4] K. Lunze, T. Singh, M. Walter, M. D. Brendel and S. Leonhardt, *"Blood glucose control algorithms for type 1 diabetic patients: A methodological review"*, Biomedical signal processing and control, vol. 8, n. 2, pp. 107-119, 2013.

[5] T. M. Gross, D. Kayne, A. King, C. Rother and S. Juth, *"A bolus calculator is an effective means of controlling postprandial glycemia in patients on insulin pump therapy"*, Diabetes technology and therapeutics, vol. 5, n. 3, pp. 365-369, 2003.

[6] G. Cappon, M. Vettoretti, G. Sparacino and A. Facchinetti, *"Continuous glucose monitoring sensors for diabetes management: a review of technologies and applications"*, Diabetes and metabolism journal, vol. 43, n. 4, pp. 383-397, 2019.

[7] S. Zavitsanou, A. Mantalaris, M. C. Georgiadis and E. N. Pistikopoulos, *"In silico closed-loop control validation studies for optimal insulin delivery in type 1 diabetes"*, IEEE transactions on biomedical engineering, vol. 62, n. 10, pp. 2369-2378, 2015.

[8] C. Cobelli, E. Renard and B. P. Kovatchev, *"Artificial pancreas: past, present, future"*, Diabetes, vol. 60, n. 11, pp. 2672-2682, 2011.

[9] D. Shi, S. Deshpande, E. Dassau and F. J. Doyle III, *"Feedback control algorithms for automated glucose management in T1DM: the state of the art"*, The artificial pancreas, pp. 1-27, 2019.

[10] R. Mauseth, I. B. Hirsch, J. Bollyky, R. Kircher, D. Matheson, S. Sanda and C. Greenbaum, *"Use of a "fuzzy logic" controller in a closed-loop artificial pancreas"*, Diabetes technology and therapeutics, vol. 15, n. 8, pp. 628-633, 2013.

[11] L. M. Huyett, E. Dassau, H. C. Zisser and F. J. Doyle III, *"Design and evaluation of a robust PID controller for a fully implantable artificial pancreas"*, Industrial & engineering chemistry research, vol. 54, n. 42, pp. 10311-10321, 2015.

[12] R. Hovorka, V. Canonico, L. J. Chassin, U. Haueter, M. Massi-Benedetti, M. O. Federici and M. E. Wilinska, *"Nonlinear model predictive control of glucose concentration in subjects with type 1 diabetes"*, Physiological measurement, vol. 25, n. 4, p. 905, 2004.

[13] C. Toffanin, M. Messori, F. Di Palma, G. De Nicolao, C. Cobelli and L. Magni, *"Artificial pancreas: model predictive control design from clinical experience"*, Journal of diabetes science and technology, vol. 7, n. 6, pp. 1470-1483, 2013.

[14] X. Sun, M. Rashid, N. Hobbs, R. Brandt, M. R. Askari and A. Cinar, *"Incorporating prior information in adaptive model predictive control for multivariable artificial pancreas systems"*, Journal of Diabetes Science and Technology, vol. 16, n. 1, pp. 19-28, 2022.

[15] N. Taleb, S. Tagougui and R. Rabasa-Lhoret, *"Single-hormone artificial pancreas use in diabetes: clinical efficacy and remaining challenges"*, Diabetes Spectrum, vol. 32, n. 3, pp. 205-208, 2019.

[16] G. Quiroz, *"The evolution of control algorithms in artificial pancreas: A historical perspective"*, Annual Reviews in Control, vol. 48, pp. 222-232, 2019.

[17] J. Pavan, D. Salvagnin, A. Facchinetti, G. Sparacino and S. Del Favero, *"Incorporating Sparse and Quantized Carbohydrates Suggestions in Model Predictive Control for Artificial Pancreas in Type 1 Diabetes"*, IEEE Transactions on Control Systems Technology, vol. 31, no. 2, pp. 570-586, 2023.

[18] T. Peyser, E. Dassau, M. Breton and J. S. Skyler, *"The artificial pancreas: current status and future prospects in the management of diabetes"*, Annals of the New York Academy of Sciences, vol. 1311, n. 1, pp. 102-123, 2014.

[19] K. Turksoy, I. Hajizadeh, S. Samad, J. Feng, M. Sevil, M. Park and A. Cinar, *"Real-time insulin bolusing for unannounced meals with artificial pancreas"*, Control Engineering Practice, vol. 59, pp. 159-164, 2017.

[20] C. Dalla Man, F. Micheletto, D. Lv, M. Breton, B. P. Kovatchev and C. Cobelli, *"The UVA/PADOVA type 1 diabetes simulator: new features"*, Journal of diabetes science and technology, vol. 8, n. 1, pp. 26-34, 2014.

[21] R. Visentin, E. Campos-Náñez, M. Schiavon, D. Lv, M. Vettoretti, M. Breton and C. Cobelli, *"The UVA/Padova type 1 diabetes simulator goes from single meal to single day",* Journal of diabetes science and technology, vol. 12, n. 2, pp. 273-281, 2018.

[22] M. Vettoretti, A. Facchinetti, G. Sparacino and C. Cobelli, *"Type-1 diabetes patient decision simulator for in silico testing safety and effectiveness of insulin treatments"*, IEEE Transactions on Biomedical Engineering, vol. 65, n. 6, pp. 1281-1290, 2017.

[23] K. S. Holkar and L. M. Waghmare, *"An overview of model predictive control"*, International Journal of control and automation, vol. 3, n. 4, pp. 47-63, 2010.

[24] S. Schmidt and K. Nørgaard, *"Bolus calculators"*, Journal of diabetes science and technology, vol. 8, n. 5, pp. 1035-1041, 2014.

[25] IBM, *"Ilog cplex optimization studio 12.9 user's manual"*, https://www.ibm.com/support/knowledgecenter/en/SSSA5P_12.9.0/ilog.odms.studio.help/Optimization_Studio/topics/COS_home.html, 2019.

[26] A. S. Brazeau, H. Mircescu, K. Desjardins, C. Leroux, I. Strychar, J. M. Ekoé and R. Rabasa-Lhoret, *"Carbohydrate counting accuracy and blood glucose variability in adults with type 1 diabetes"*, Diabetes research and clinical practice, vol. 99, n. 1, pp. 19-23, 2013.

[27] D. M. Maahs, B. A. Buckingham, J. R. Castle, A. Cinar, E. R. Damiano, E. Dassau and J. W. Lum, *"Outcome measures for artificial pancreas clinical trials: a consensus report"*, Diabetes care, vol. 39, n. 7, pp. 1175-1179, 2016.

[28] T. Battelino, T. Danne, R. M. Bergenstal, S. A. Amiel, R. Beck, T. Biester and M. Phillip, *"Clinical targets for continuous glucose monitoring data interpretation: recommendations from the international consensus on time in range"*, Diabetes care, vol. 42, n. 8, pp. 1593-1603, 2019.

[29] P. I. Frazier, *"A tutorial on Bayesian optimization"*, arXiv preprint arXiv:1807.02811, 2018.

[30] S. Goutelle, M. Maurin, F. Rougier, X. Barbaut, L. Bourguignon, M. Ducher and P. Maire, *"The Hill equation: a review of its capabilities in pharmacological modelling"*, Fundamental and clinical pharmacology, vol. 22, n. 6, pp. 633-648, 2008.

[31] N. Taleb, A. Haidar, V. Messier, V. Gingras, L. Legault and R. Rabasa-Lhoret, *"Glucagon in artificial pancreas systems: potential benefits and safety profile of future chronic use"*, Diabetes, Obesity and Metabolism, vol. 19, n. 1, pp. 13-23, 2017.

[32] A. Haidar, *"Insulin-and-glucagon artificial pancreas versus insulin-alone artificial pancreas: a short review"*, Diabetes Spectrum, vol. 32, n. 3, pp. 215-221, 2019.

[33] A. S. Brazeau, H. Mircescu, K. Desjardins, C. Leroux, I. Strychar, J. M. Ekoé and R. Rabasa-Lhoret, *"Carbohydrate counting accuracy and blood glucose variability in adults with type 1 diabetes"*, Diabetes research and clinical practice, vol. 99, n. 1, pp. 19-23, 2013.